

Anisotropic Growth of Crystalline Dust Grains in Protoplanetary Disks

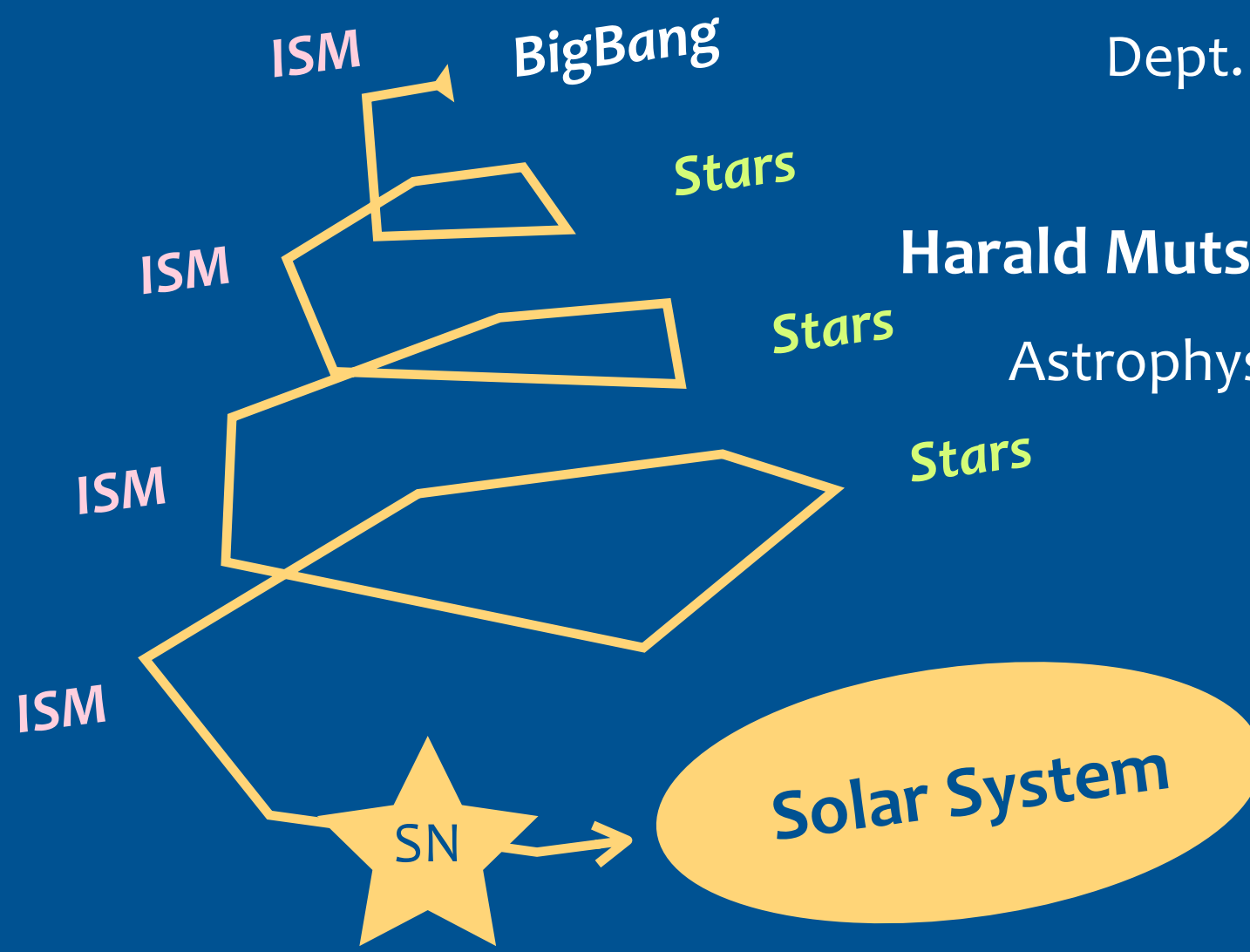
*Aki Takigawa

Shogo Tachibana, Hiroko Nagahara, Kazuhito Ozawa

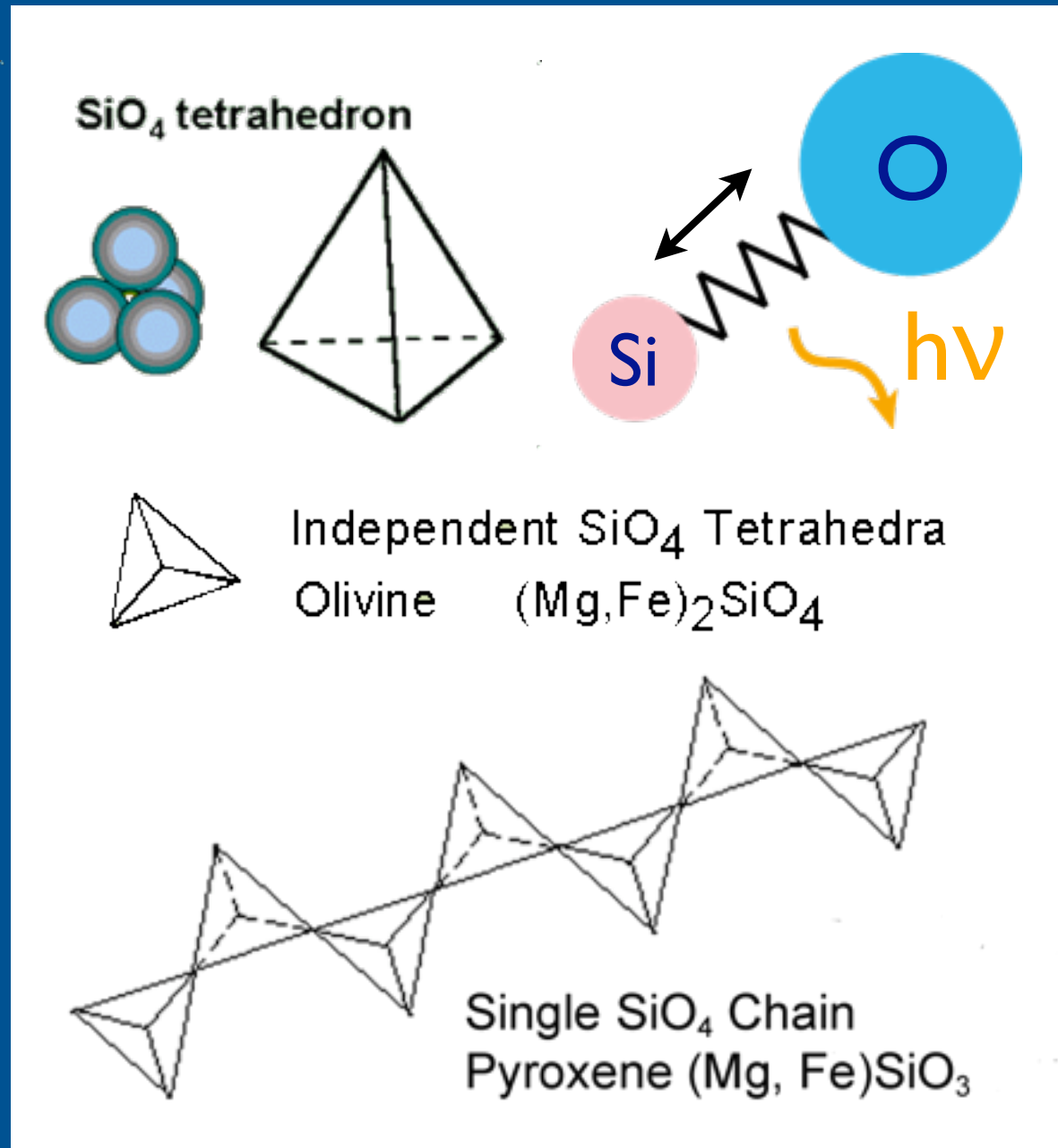
Dept. Earth and Planetary Science, Univ. Tokyo

Harald Mutschke, Akemi Tamanai, Simon Zeidler

Astrophysical Institute and University Observatory
- Friedrich-Schiller University Jena



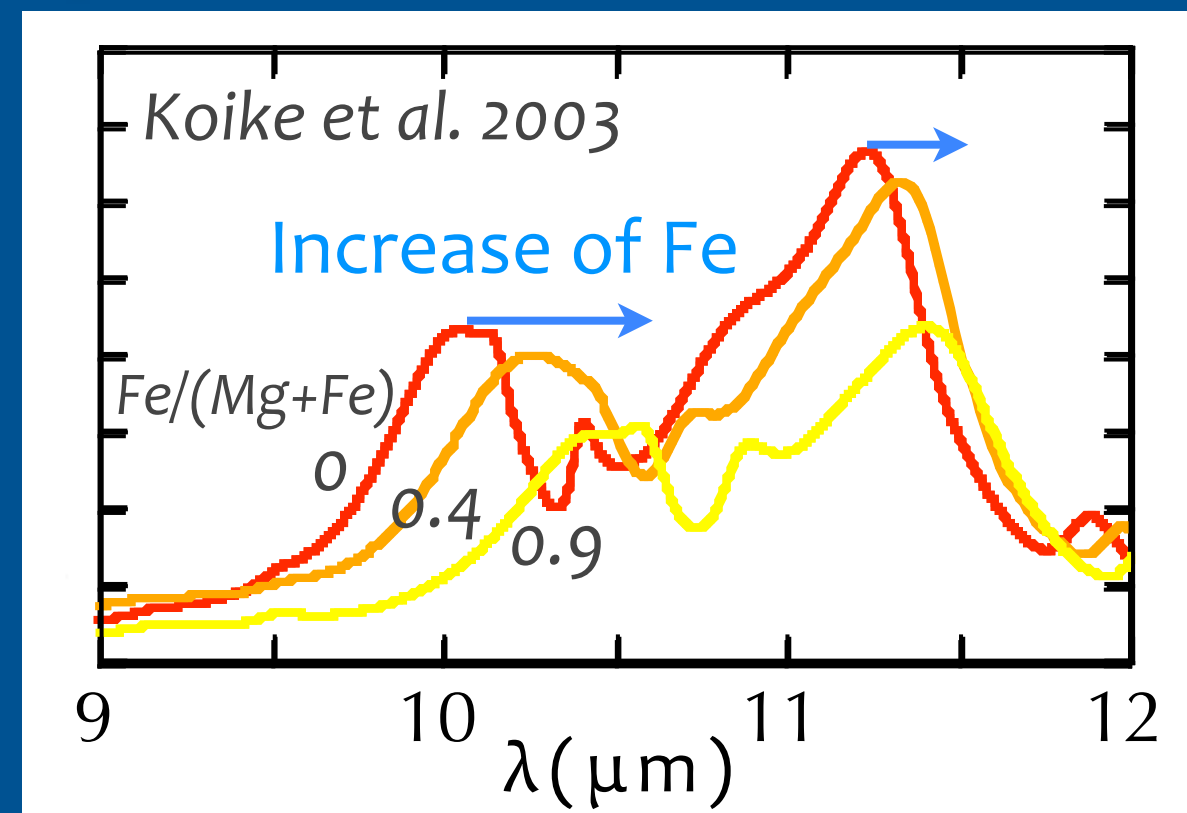
Infrared Spectrum



Spectra of dust grains depend on

- arrangement of atoms
- temperature, composition, size, shape

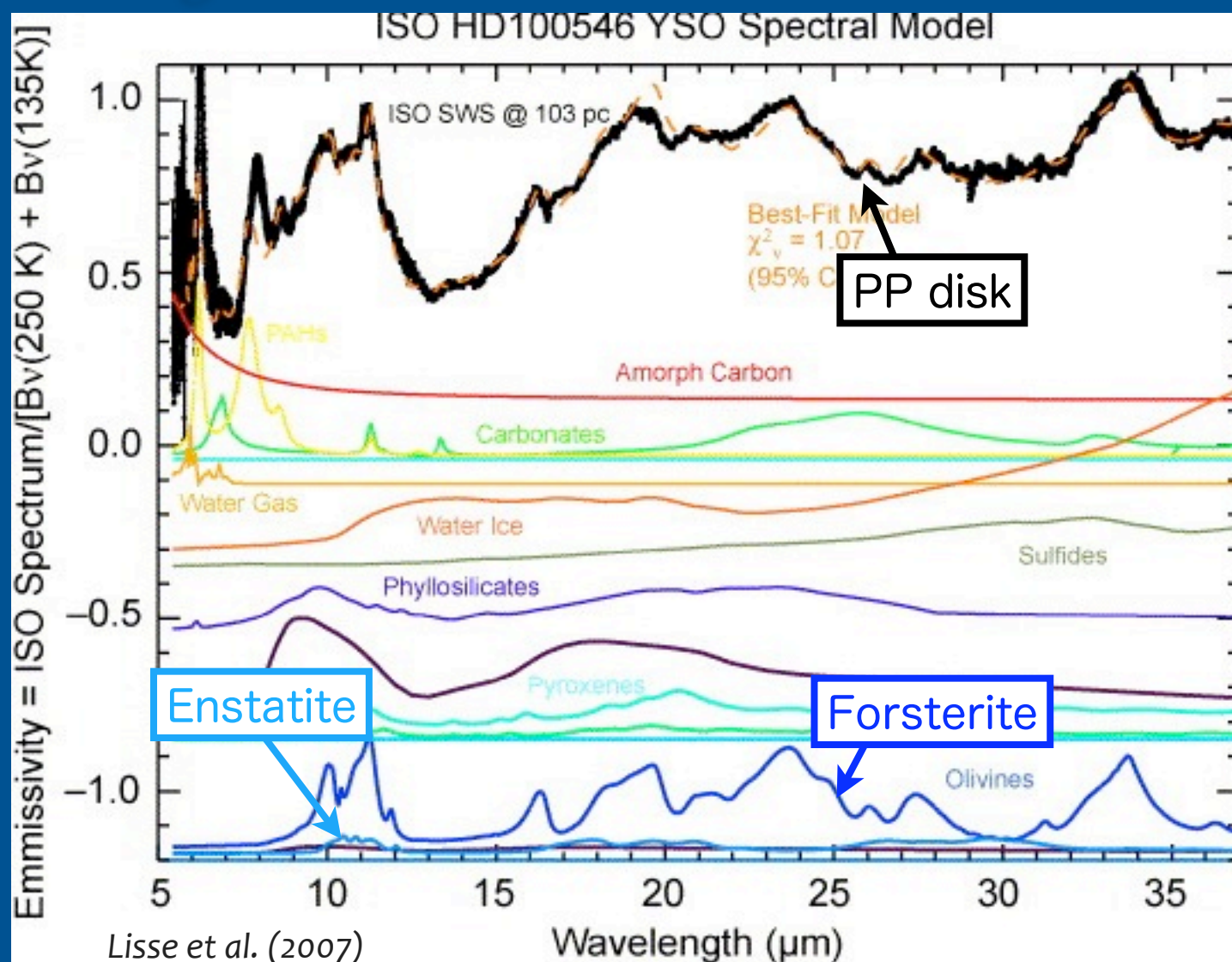
e.g., Fo spectrum depends on Fe content



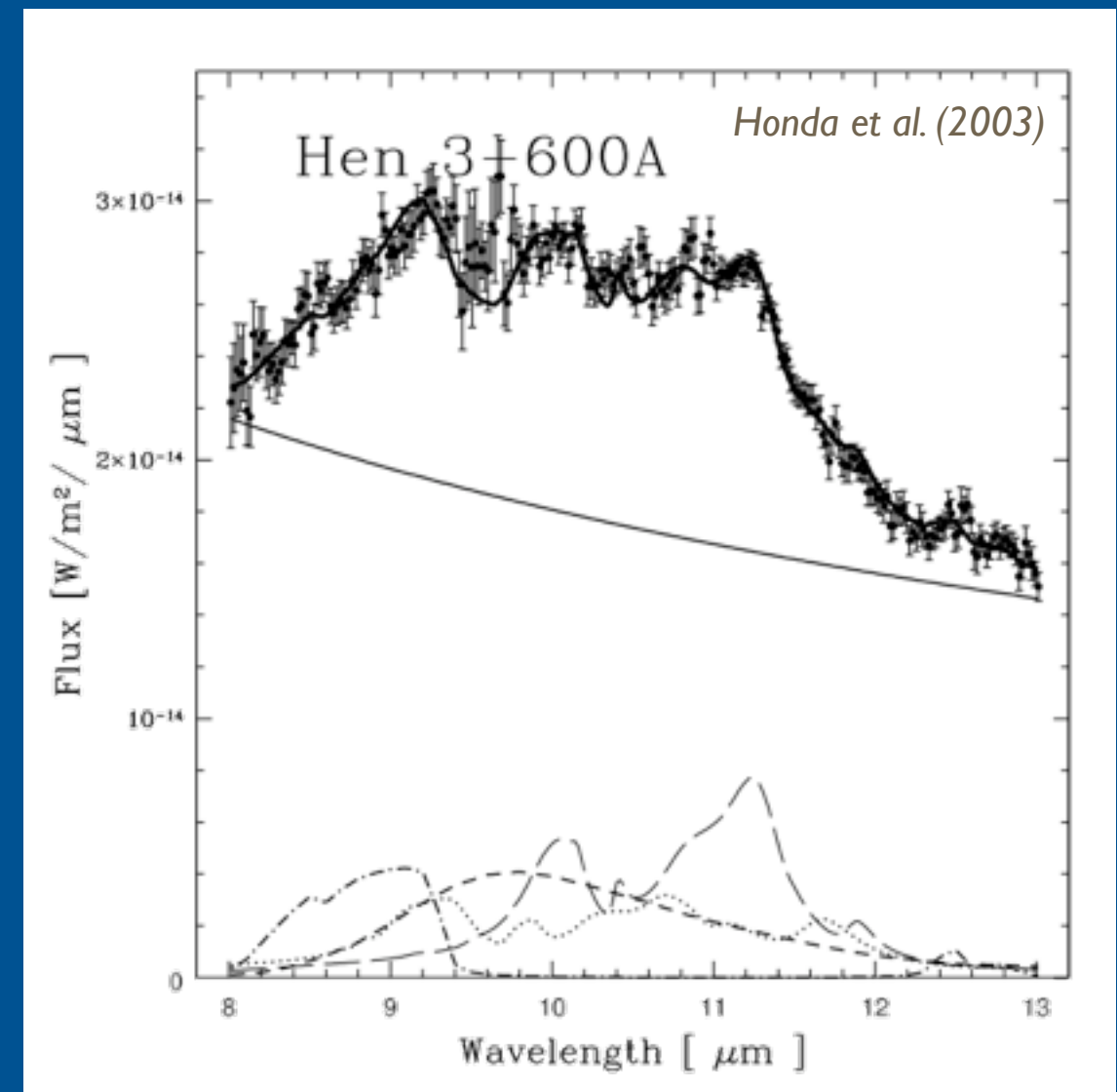
Koike et al. 1993, 1995, 2003, 2006, Fabian et al. 2001, Jäger et al. 1994, 1998, Tamanai et al. 2006, 2009, Murata et al. 2007

Observation & Laboratory spectra

Herbig AeBe star



T-Tauri star



Dust: Amorphous silicates, Forsterite, Enstatite, Oxides, H₂O ice, ...
--> Crystal / Amorphous, Chemical compositions, Size, ...

Motivation

Understanding of dust formation processes and/or conditions from observed spectra using the relationship between dust properties & formation processes

- Dust shape and its relation to crystallographic orientation (**crystallographically anisotropic shape**)
- Dust spectra formed under circumstellar conditions

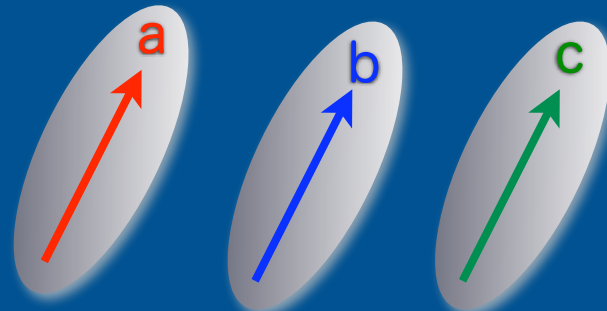
Crystallographically Anisotropic Shape



Specific shape related to a specific crystallographic orientation

- reflects crystal structure, **formation process & condition**

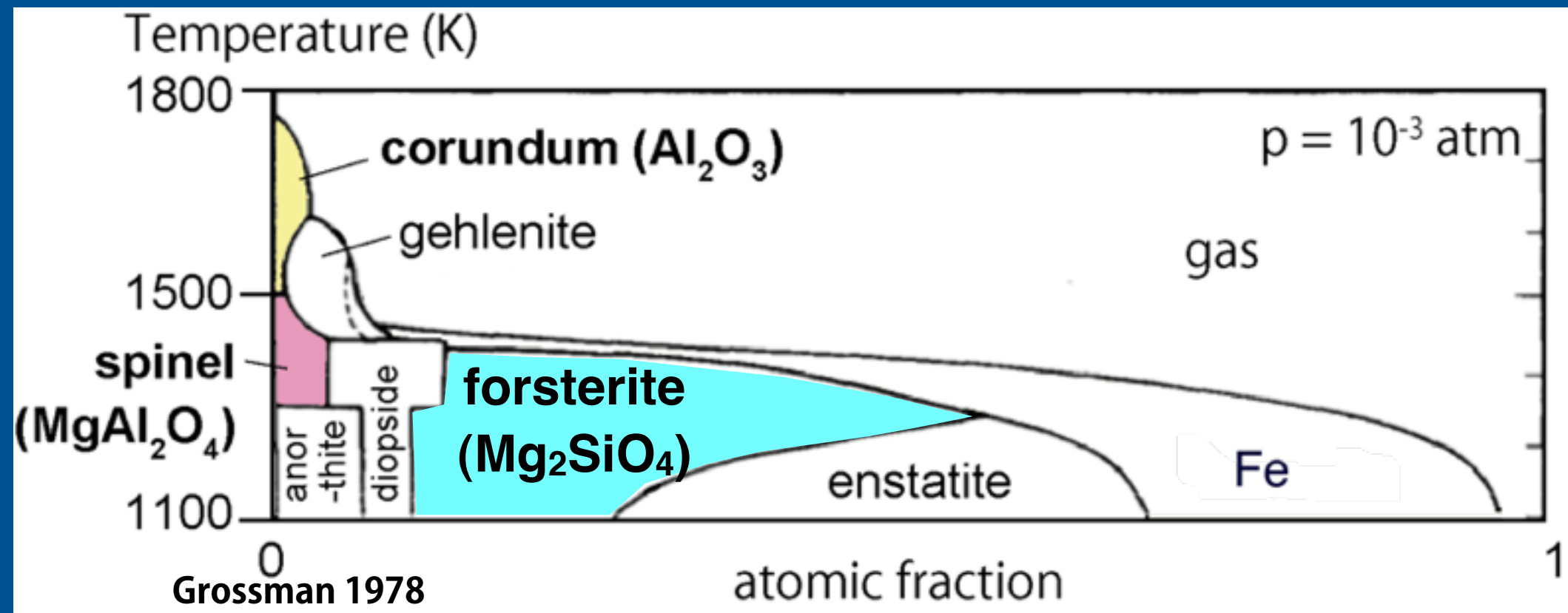
IR spectra depend on crystallographically anisotropic shape



apparently look the same, but different crystallographically anisotropic shapes

Crystallographically anisotropic shape in circumstellar environments?

Outline



1. Processes to change crystallographically anisotropic shapes

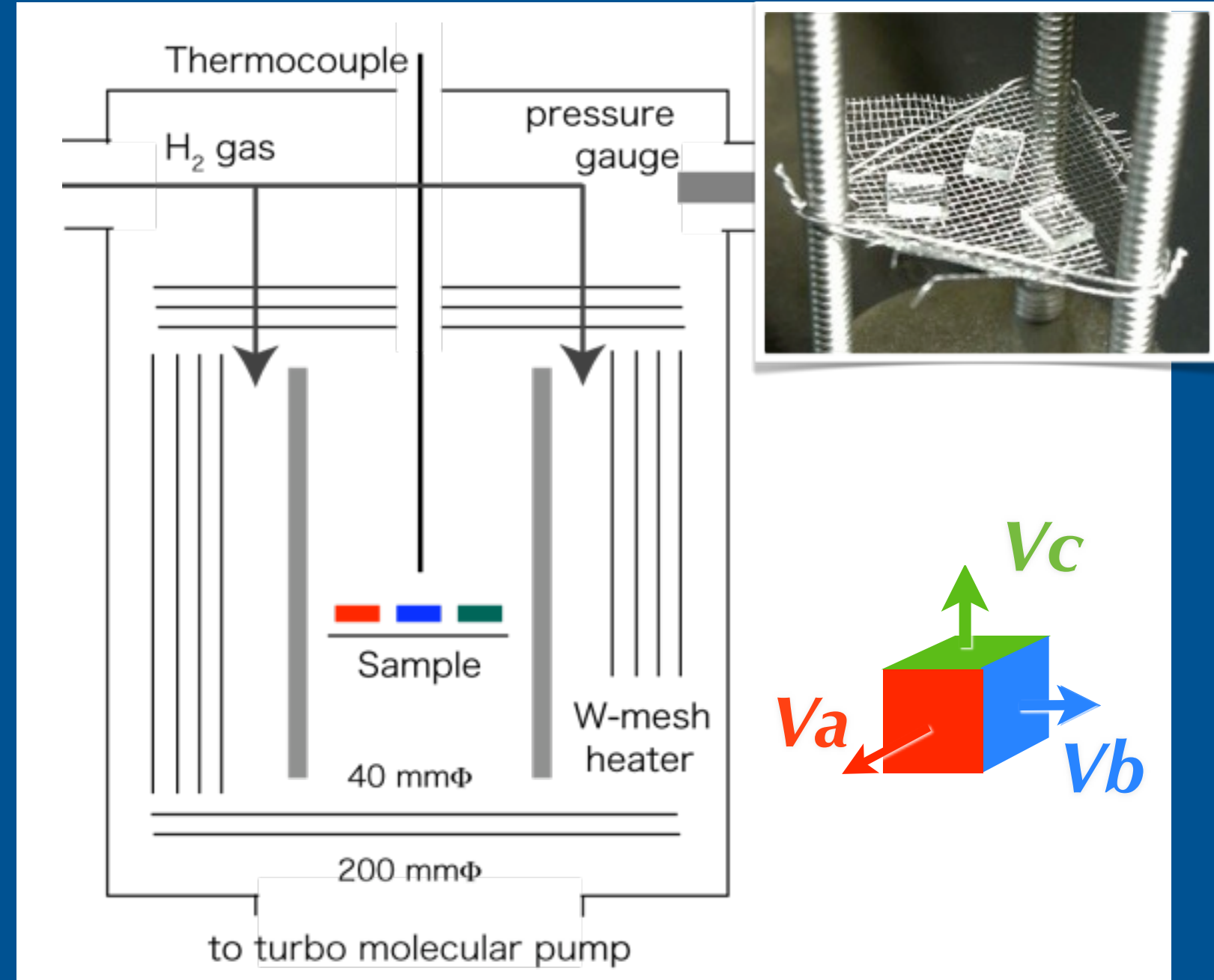
- Evaporation experiments of forsterite in H_2 gas
- Condensation experiments of corundum
- Spectra of different crystallographically anisotropic shapes

2. IR spectra of spinel formed under circumstellar conditions

Evaporation experiments of forsterite

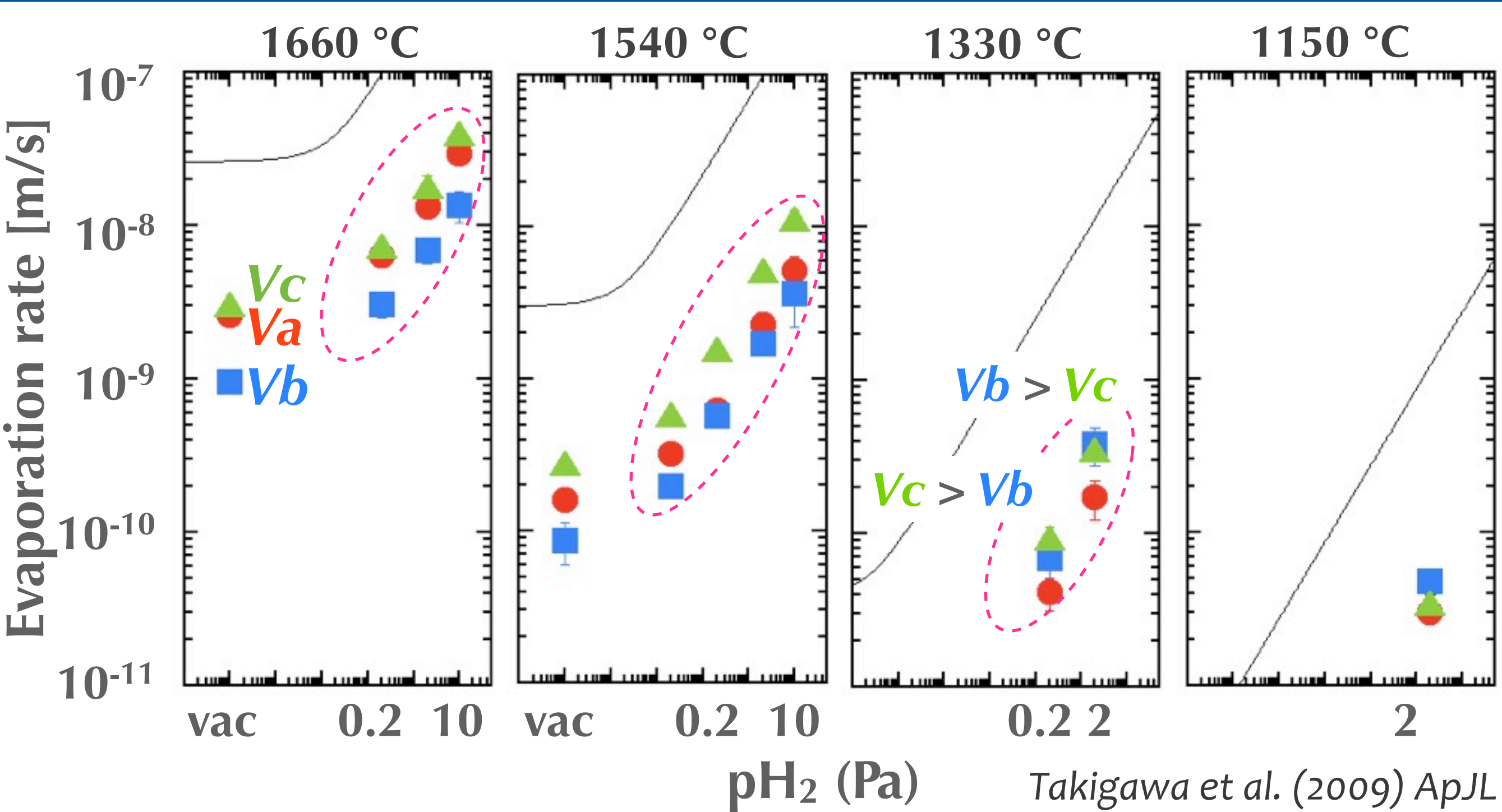


Temp: 1660-1130°C
P_{H₂}: 10⁻²-10Pa, Vacuum



Anisotropic evaporation rates along different crystallographic axes

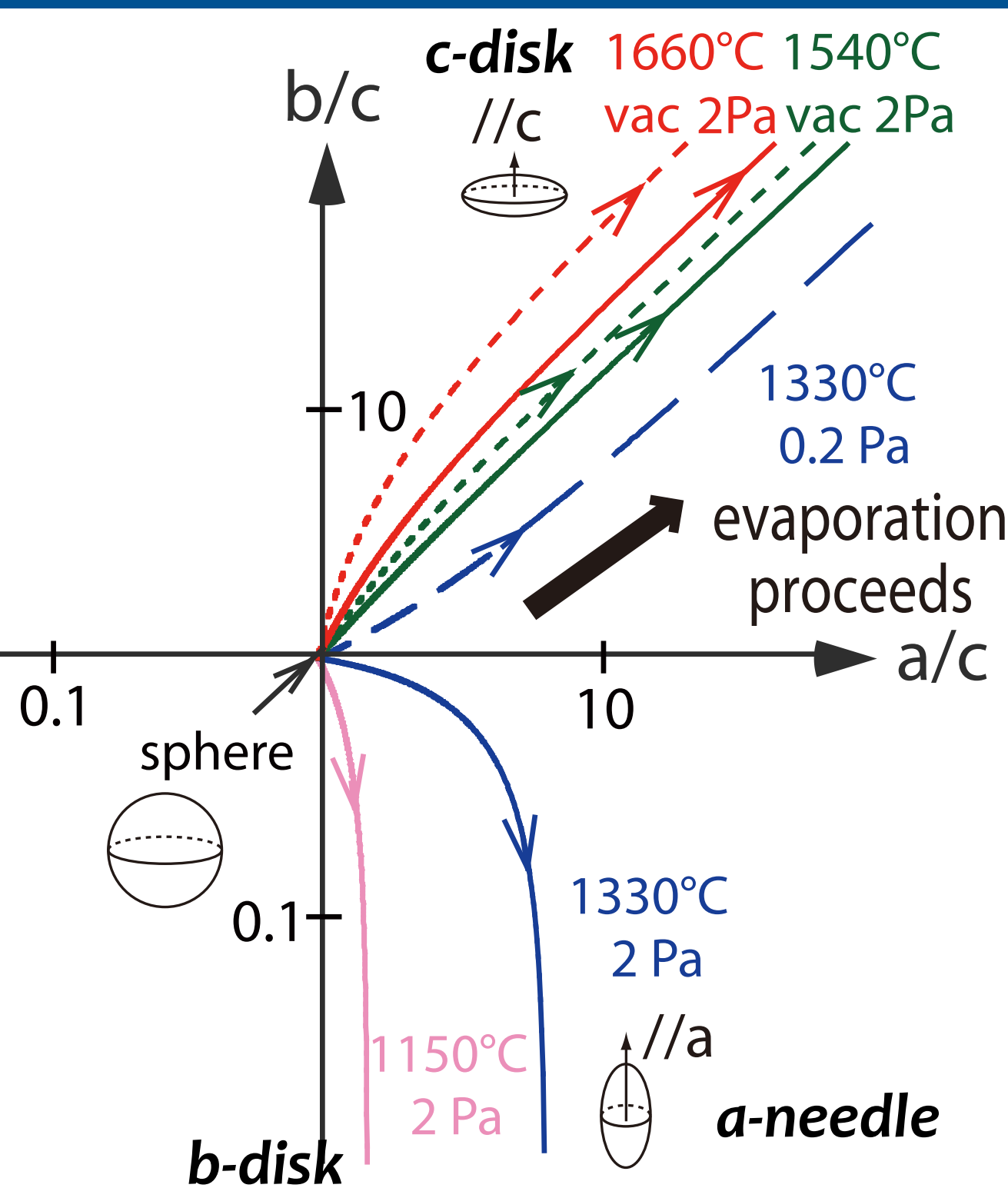
Anisotropy in evaporation rates of forsterite



Anisotropy in evaporation rates changes with T and pH₂

Shape change due to anisotropic evaporation

Evaporation from a sphere



At higher T., fastest evaporation along the c-axis

- disk flattened along the c-axis

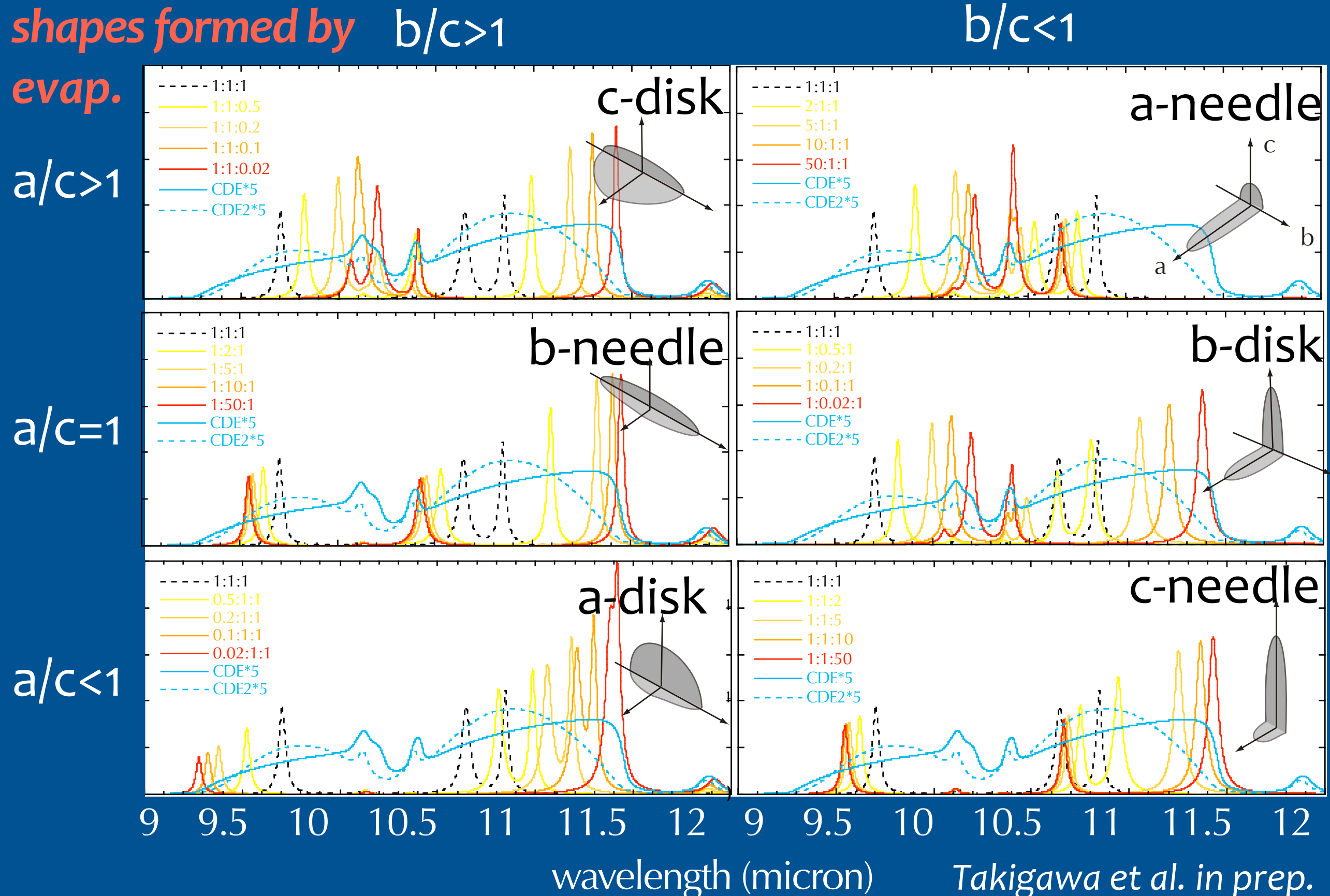
At lower T., fastest evaporation along the b-axis

- needle elongating along the a-axis
- disk flattened along the b-axis

Evaporation makes shapes only with $a/c \geq 1$

Spectral change of forsterite

shapes formed by evap.

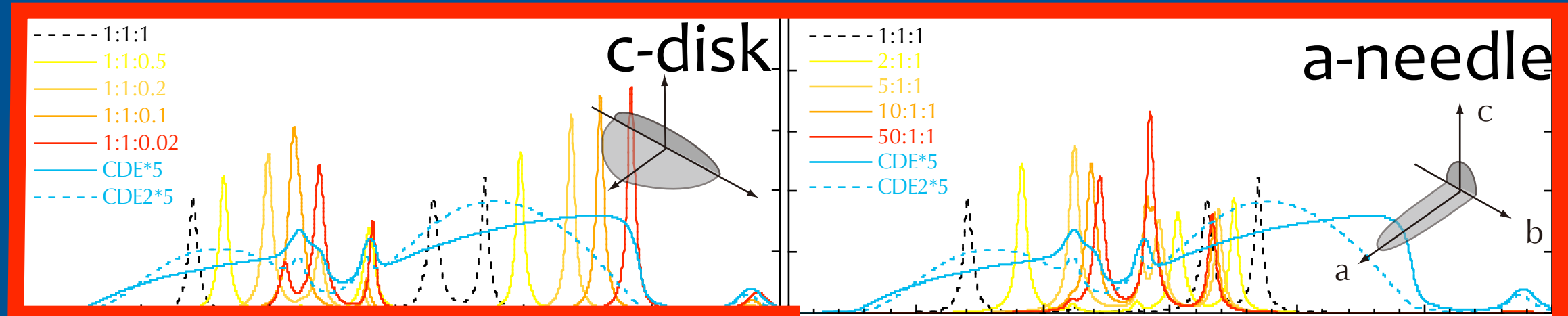


Spectral change of forsterite

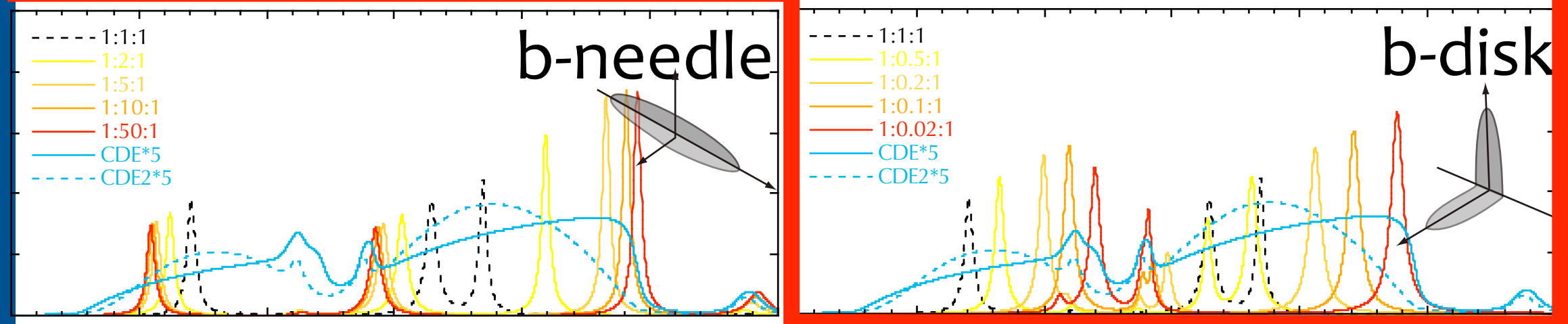
shapes formed by $b/c > 1$

evap.

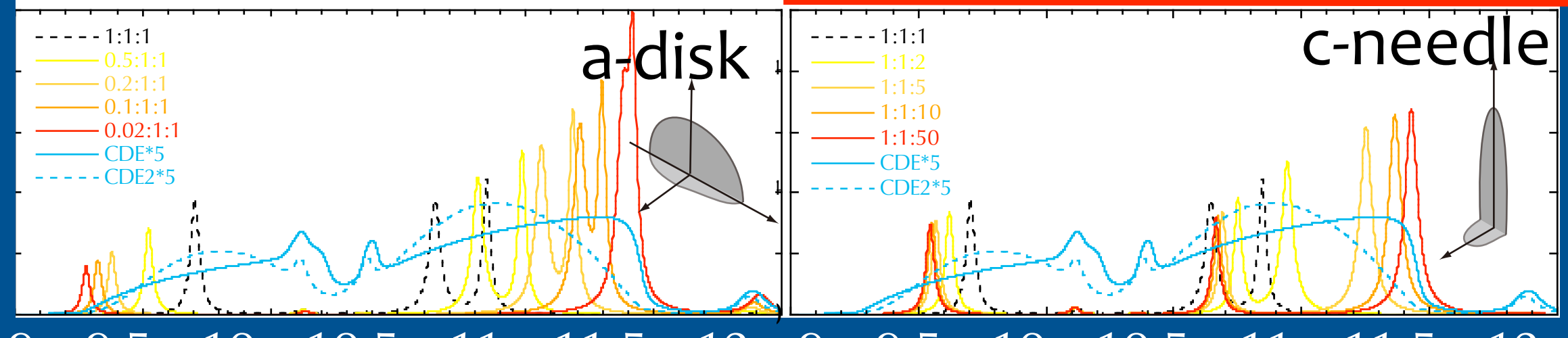
$a/c > 1$



$a/c = 1$



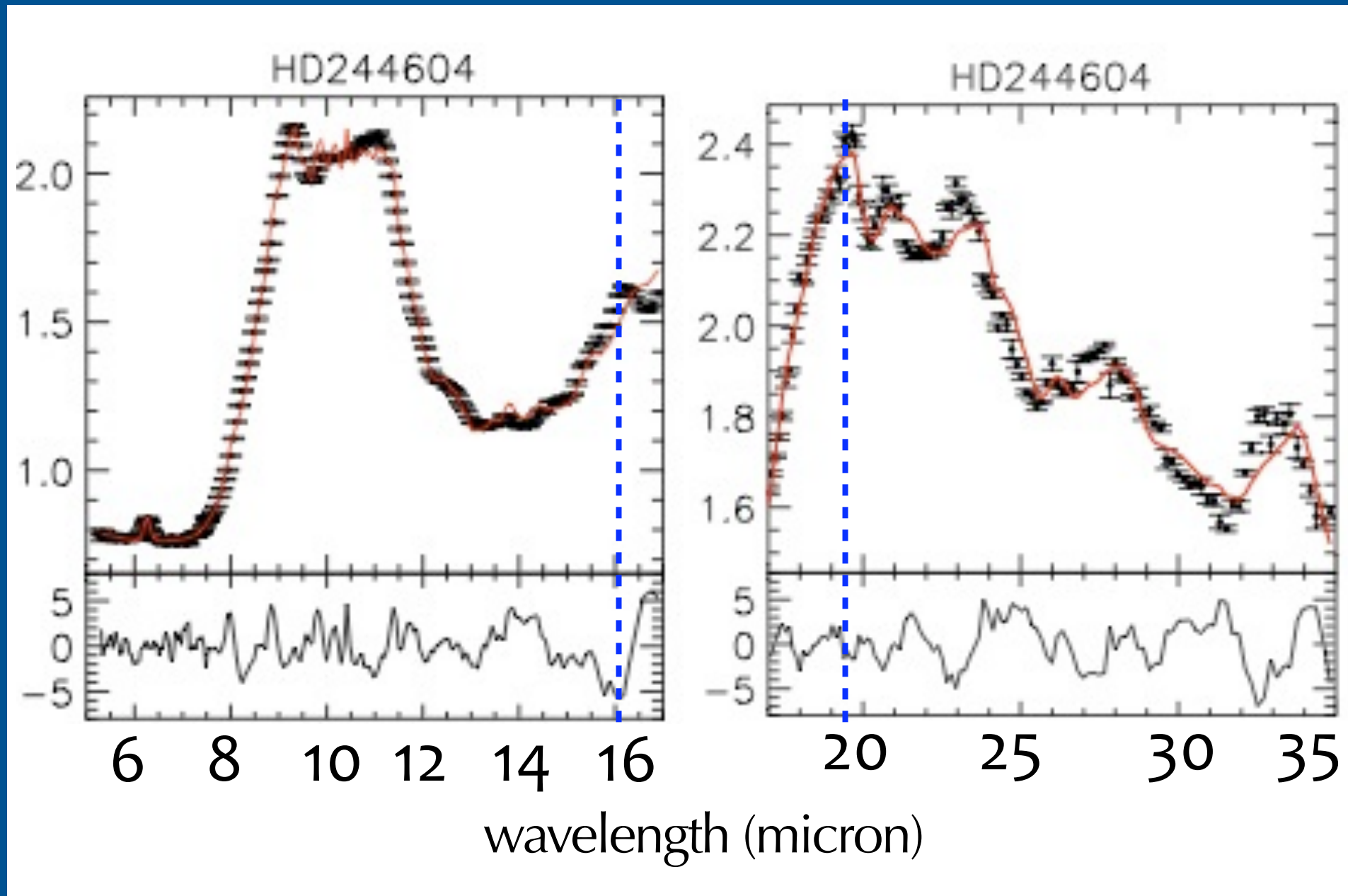
$a/c < 1$



wavelength (micron)

Takigawa et al. in prep.

16 & 19.5 micron features

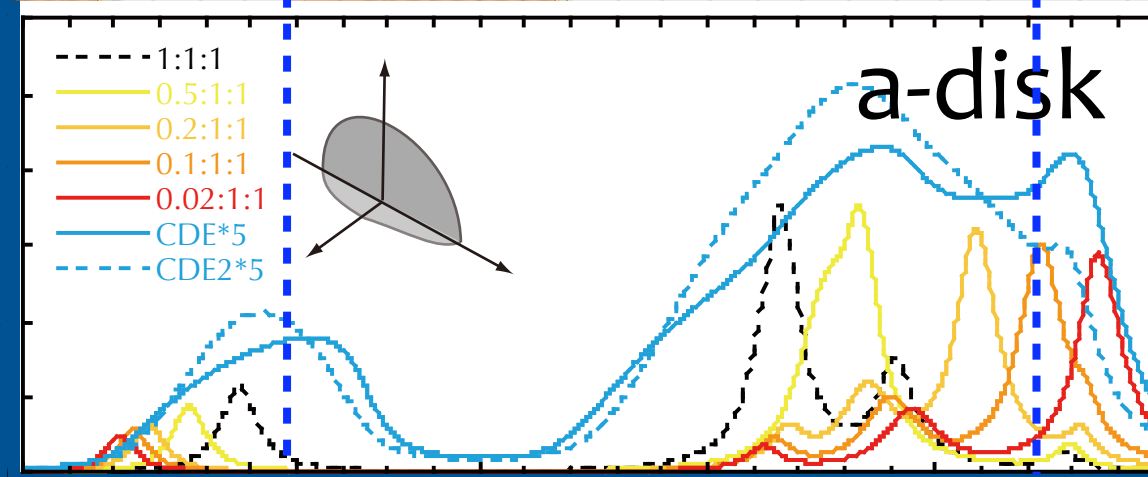
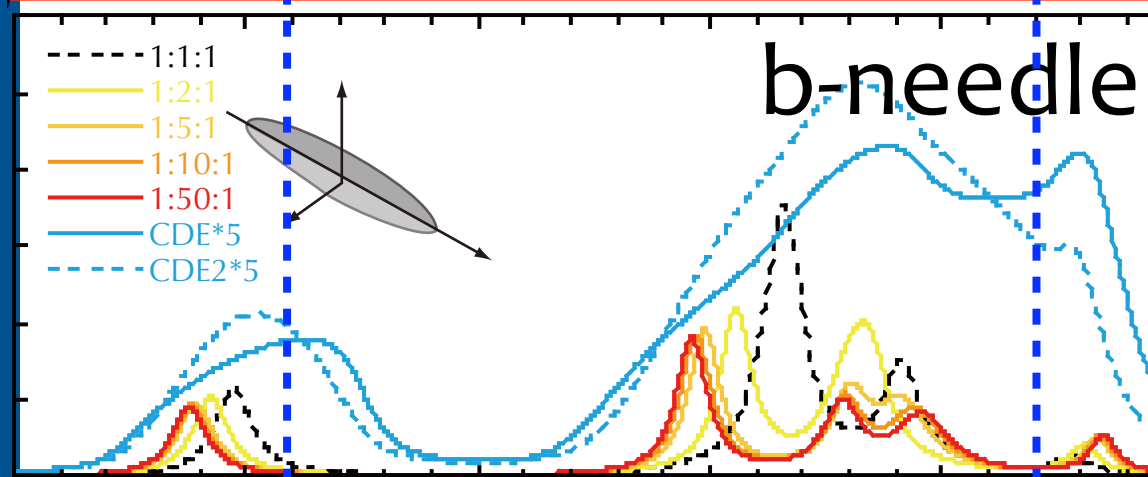
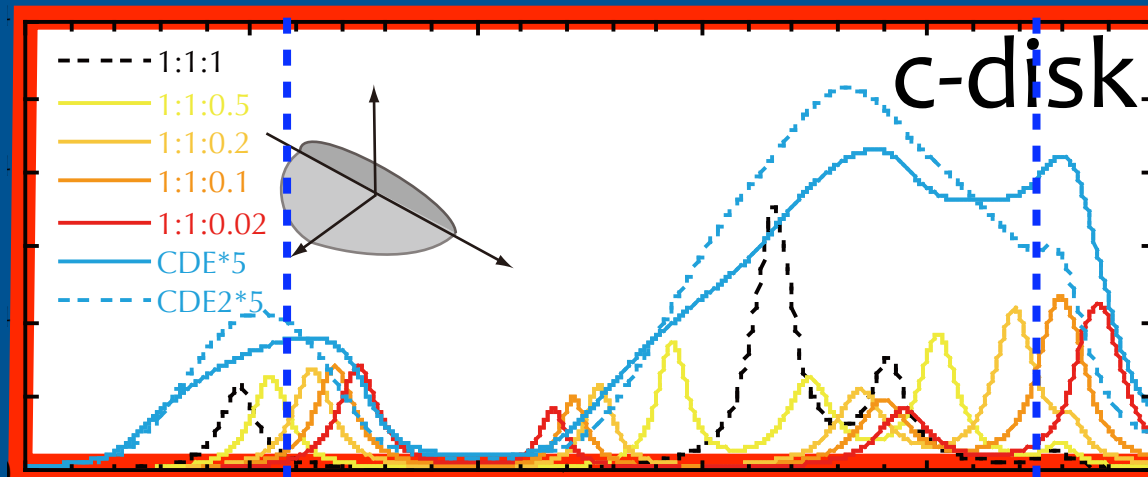


Juhász et al. 2010

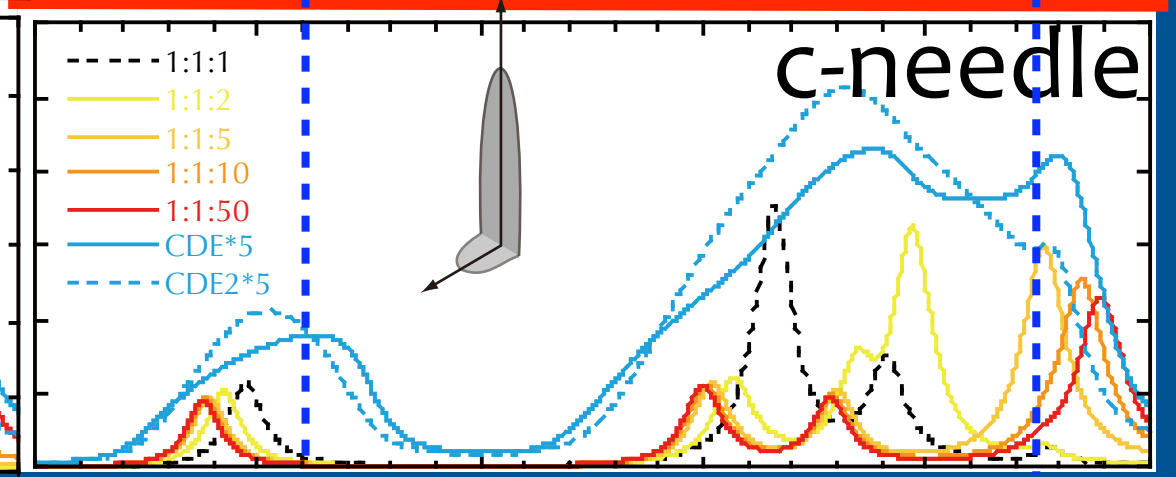
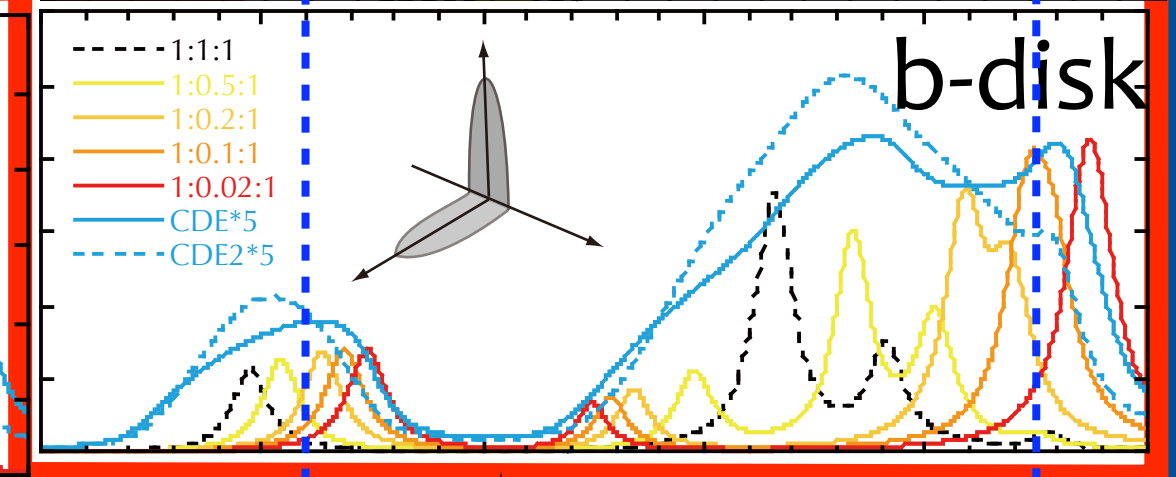
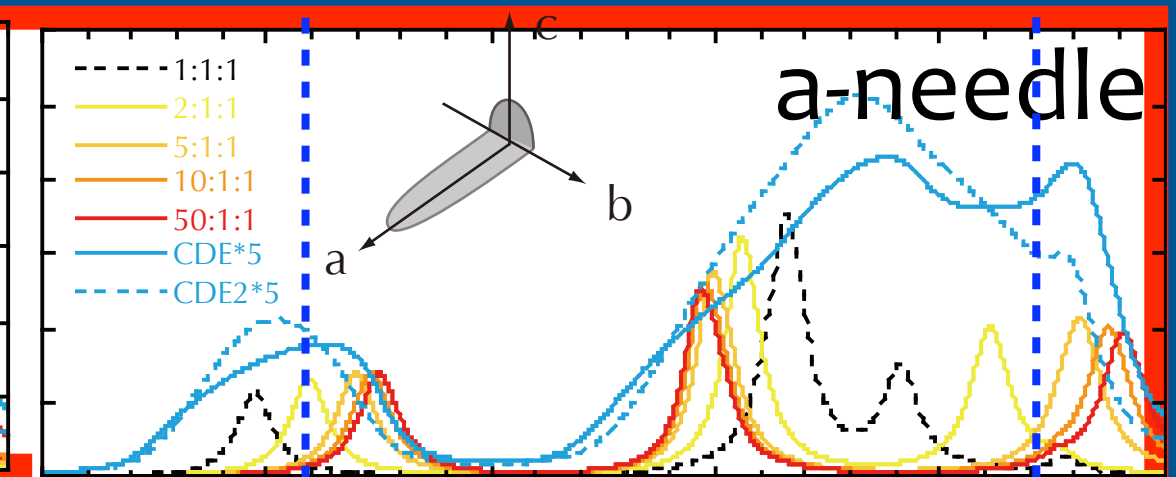
16 & 19.5 micron features

shapes formed by evap.

a/c>1



b/c<1



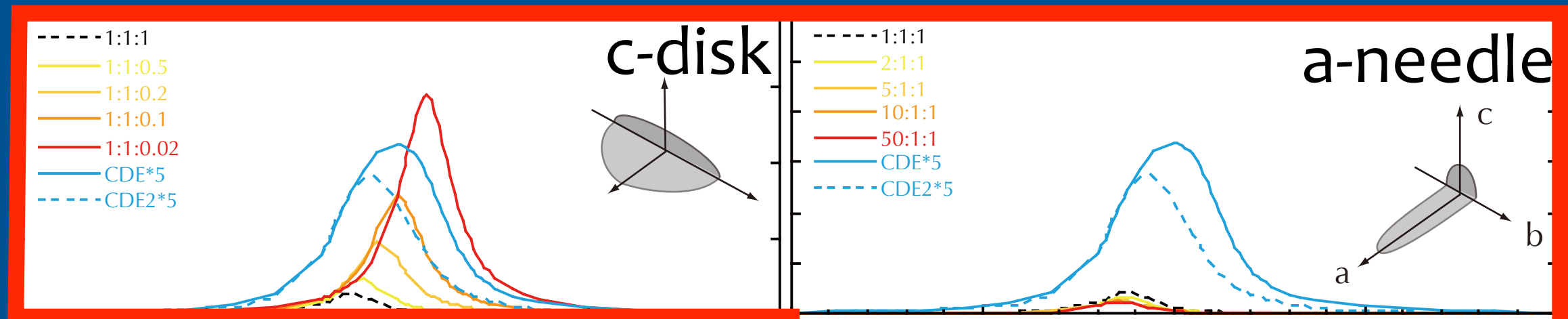
wavelength (micron)

Takigawa et al. in prep.

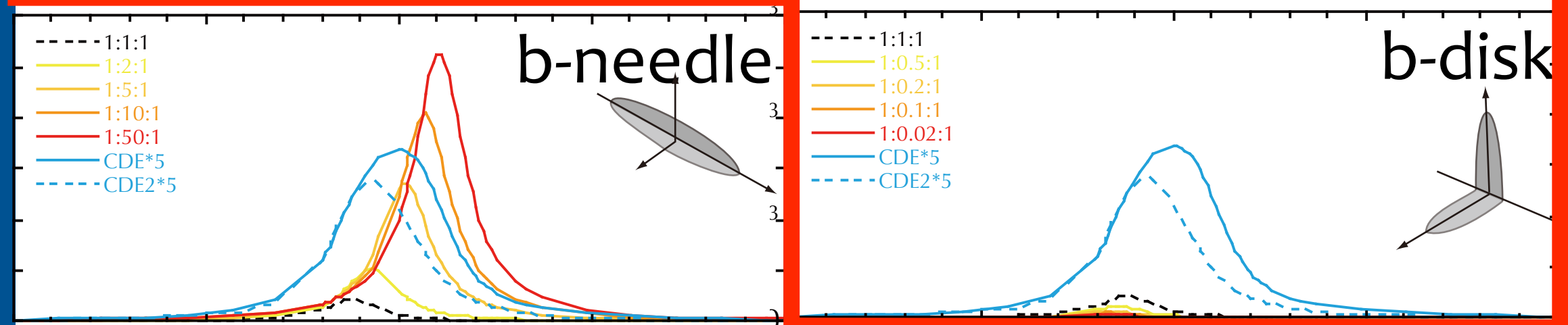
69-micron feature

shapes formed by evap.

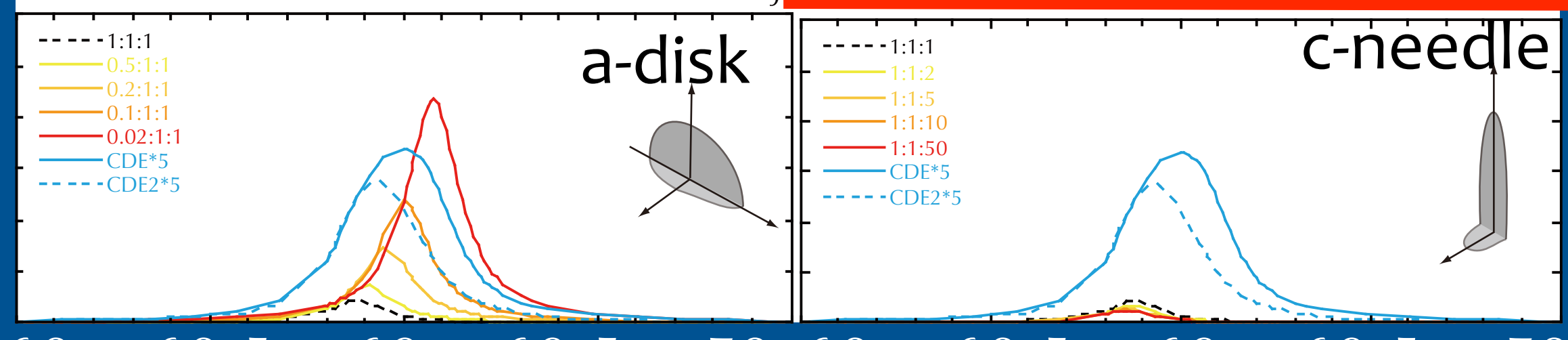
$a/c > 1$



$a/c = 1$



$a/c < 1$



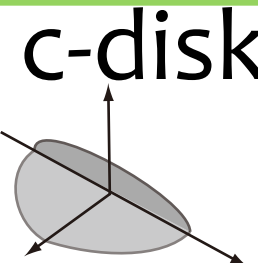
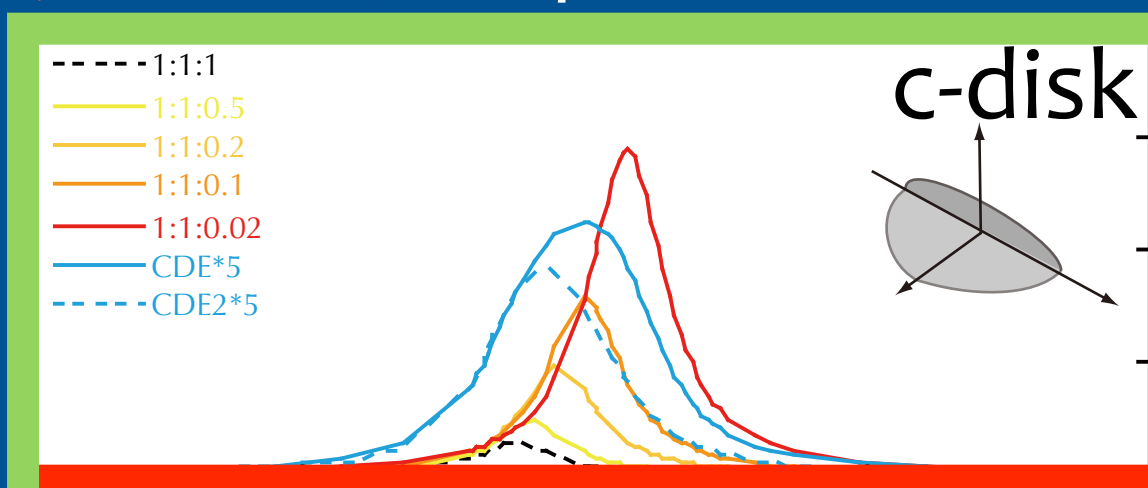
wavelength (micron)

Takigawa et al. in prep.

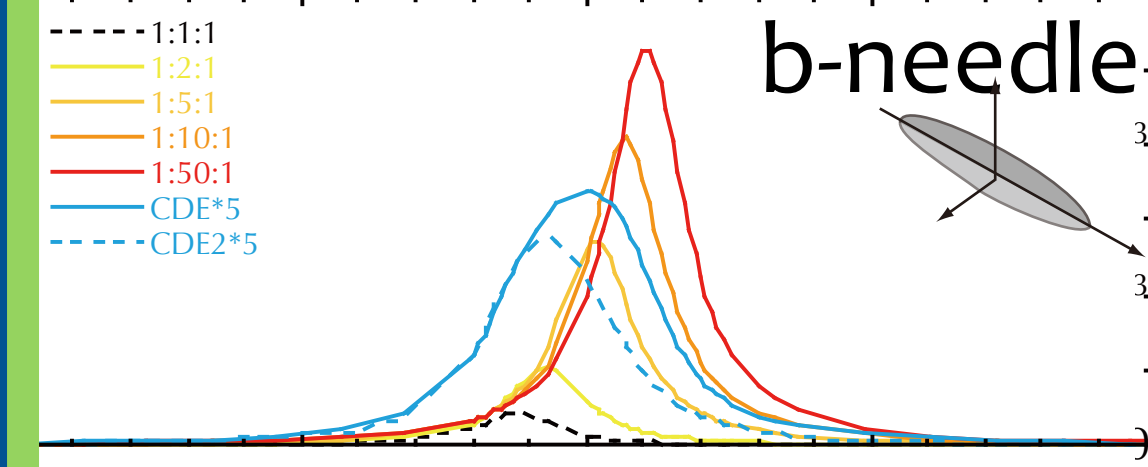
69-micron feature

*shapes formed by
evap.*

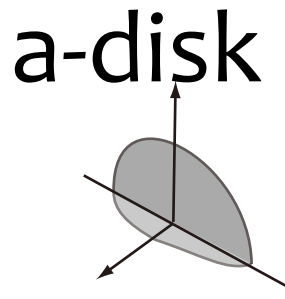
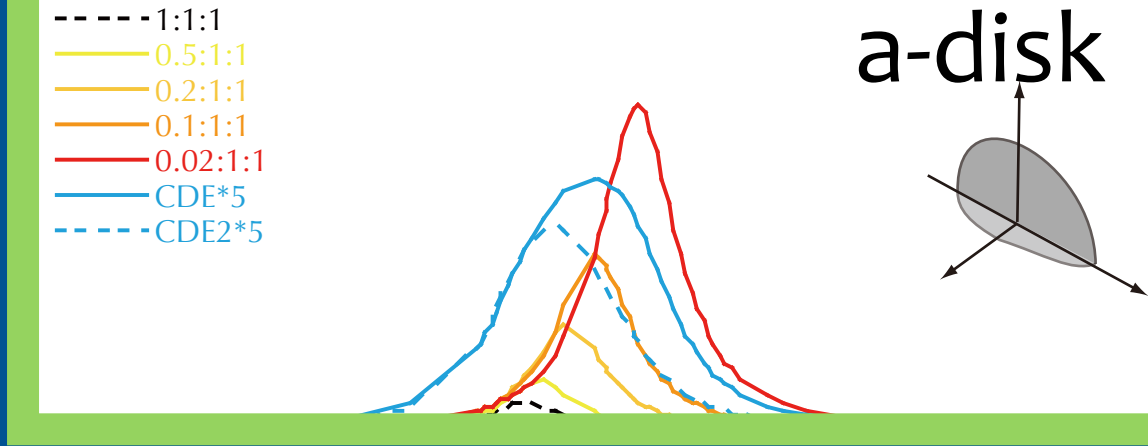
$a/c > 1$



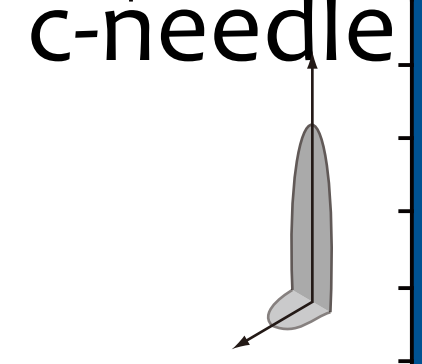
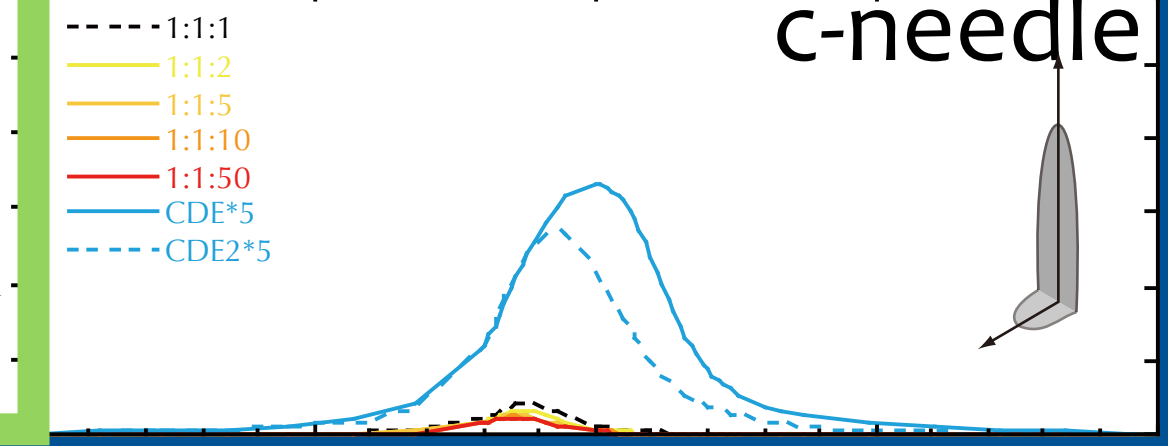
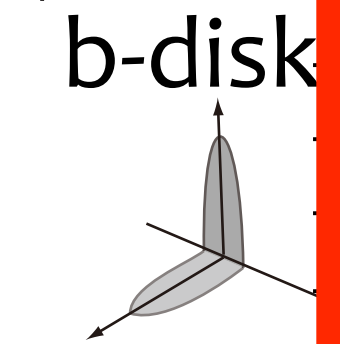
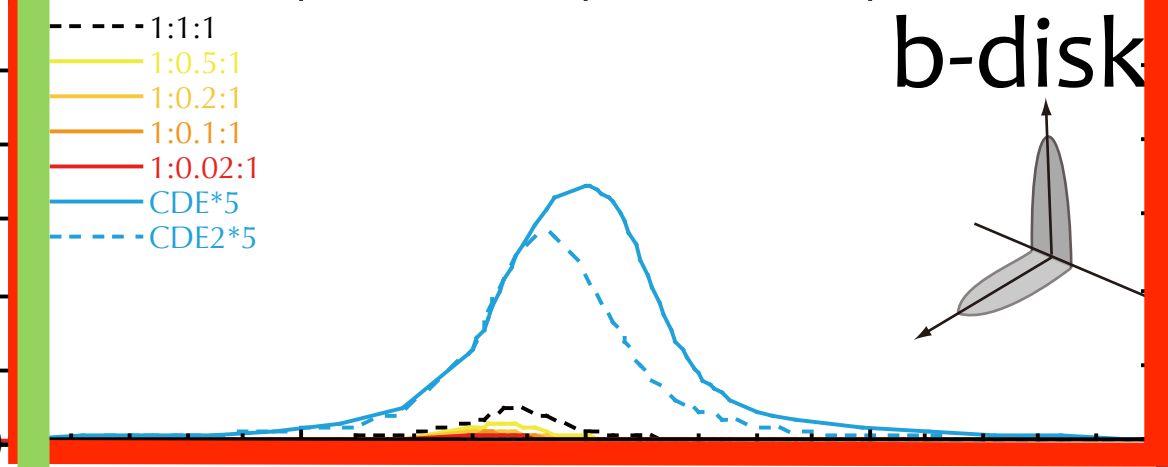
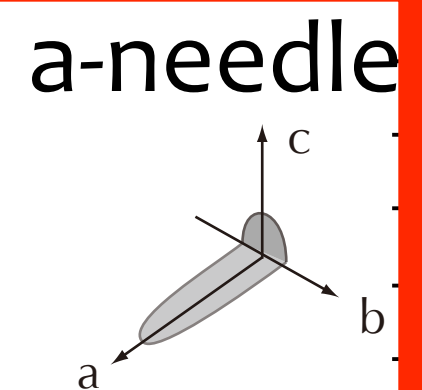
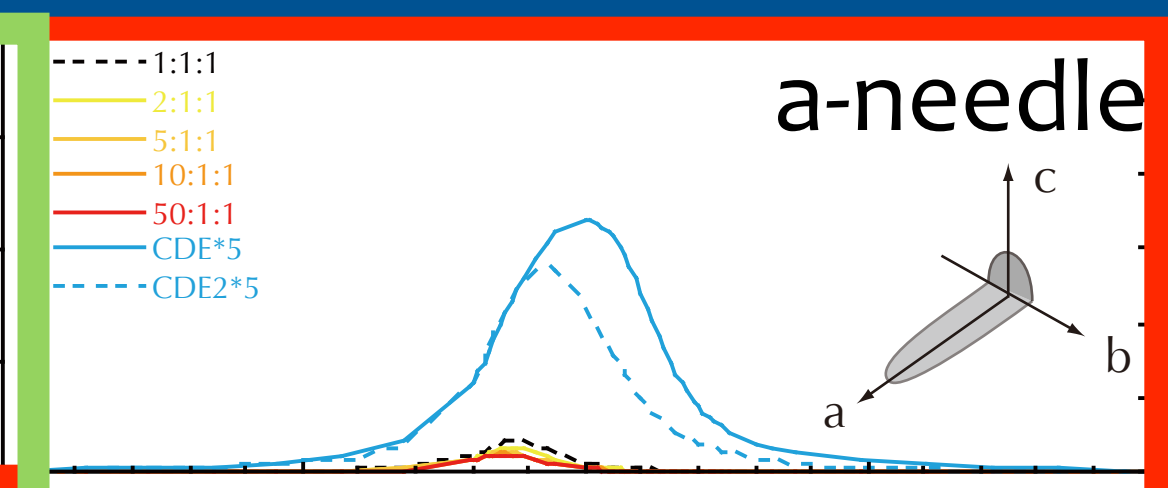
$a/c = 1$



$a/c < 1$



$b/c > 1$



wavelength (micron)

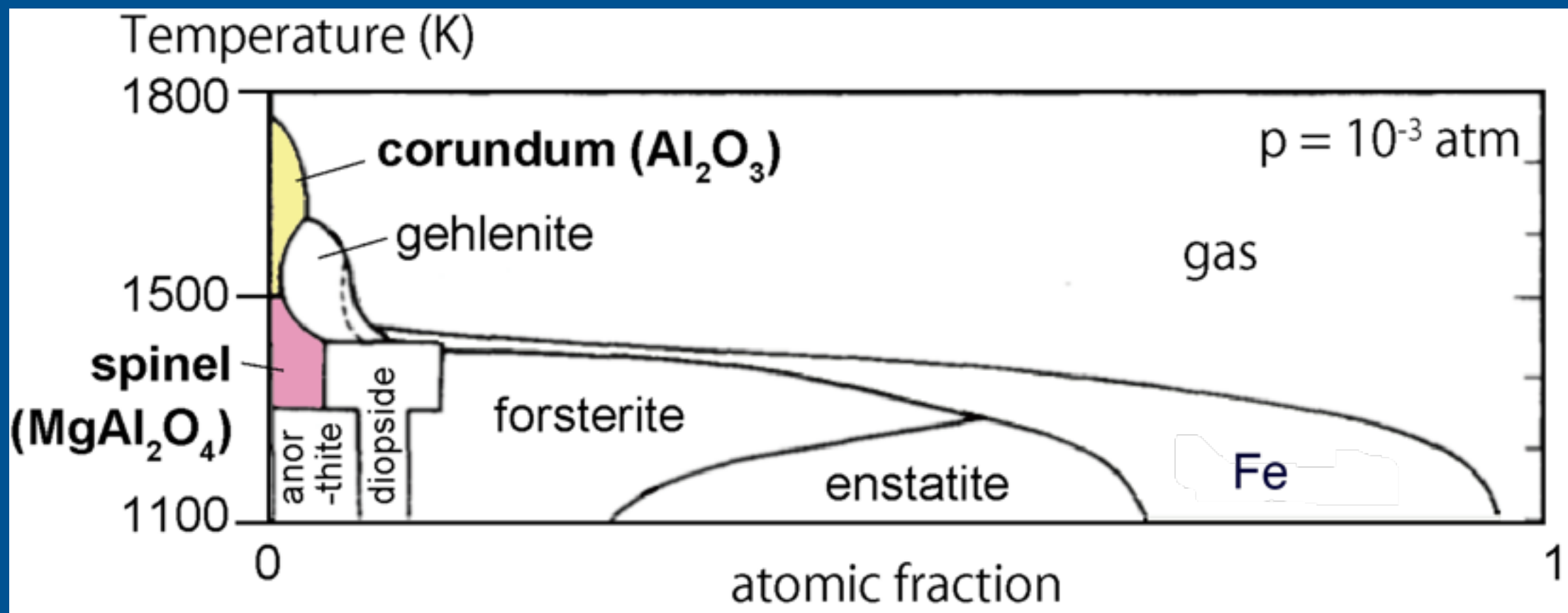
Takigawa et al. in prep.

Evaporation of forsterite

- Anisotropic
- Changes of crystallographically anisotropic shape cause observable changes of IR spectra

Corundum

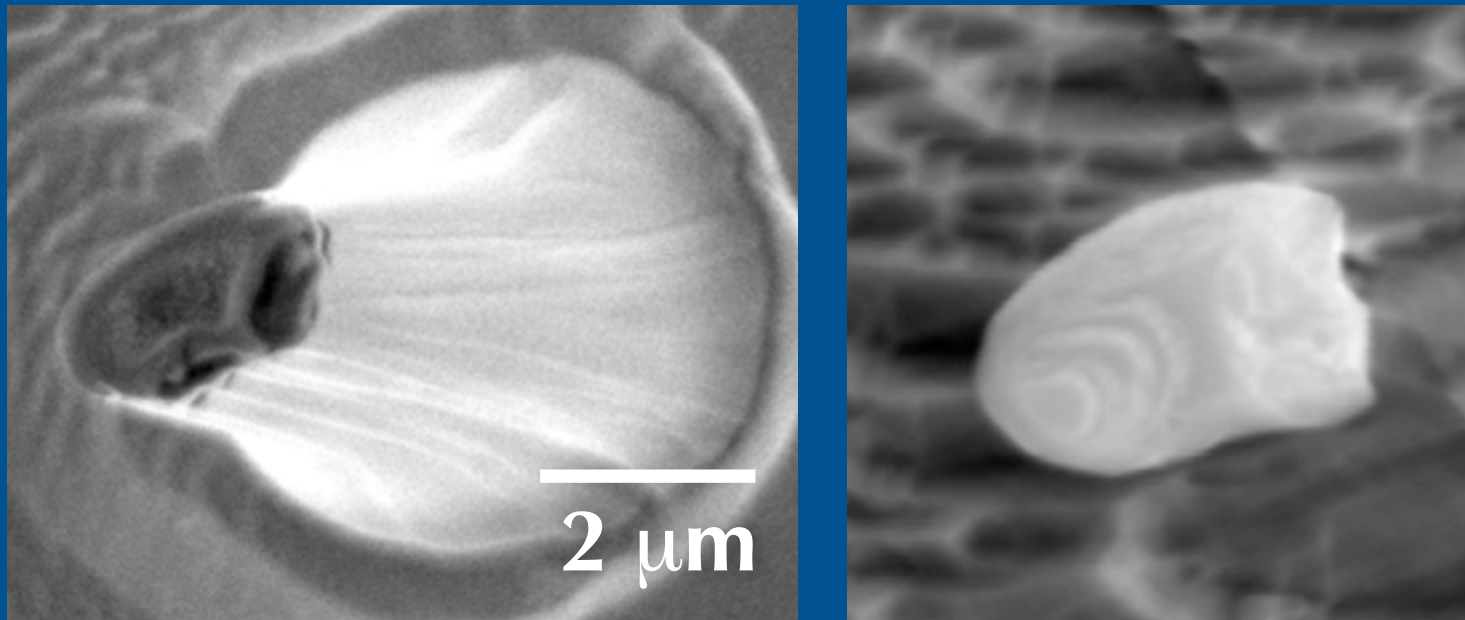
- First condensate from gas in protoplanetary disks and around O-rich AGB stars



Grossman 1978

Corundum

- Presolar & solar corundum
 - direct evidence of corundum condensation



- Astronomical observation
 - candidate for the 13 um-feature in outflows around O-rich AGB stars (e.g., Posch et al. 1999)

Condensation experiments of corundum



gas source: Al_2O_3 powder (4N+)
substrate: Mo-ribbons
crucible: Ir (>99.9%)

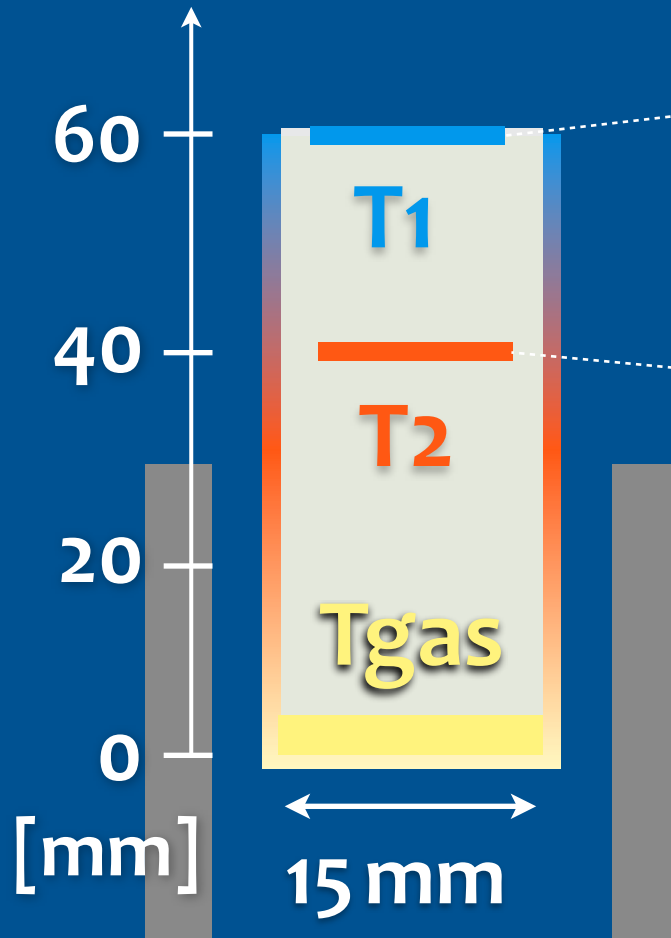


Condensation experiments of corundum



Condensation experiments of corundum

supersaturation ratio



$$p = 5 \times 10^{-5} \text{ Pa}$$

$$S1 = \frac{f_{in}}{f_{out}(T1)}$$

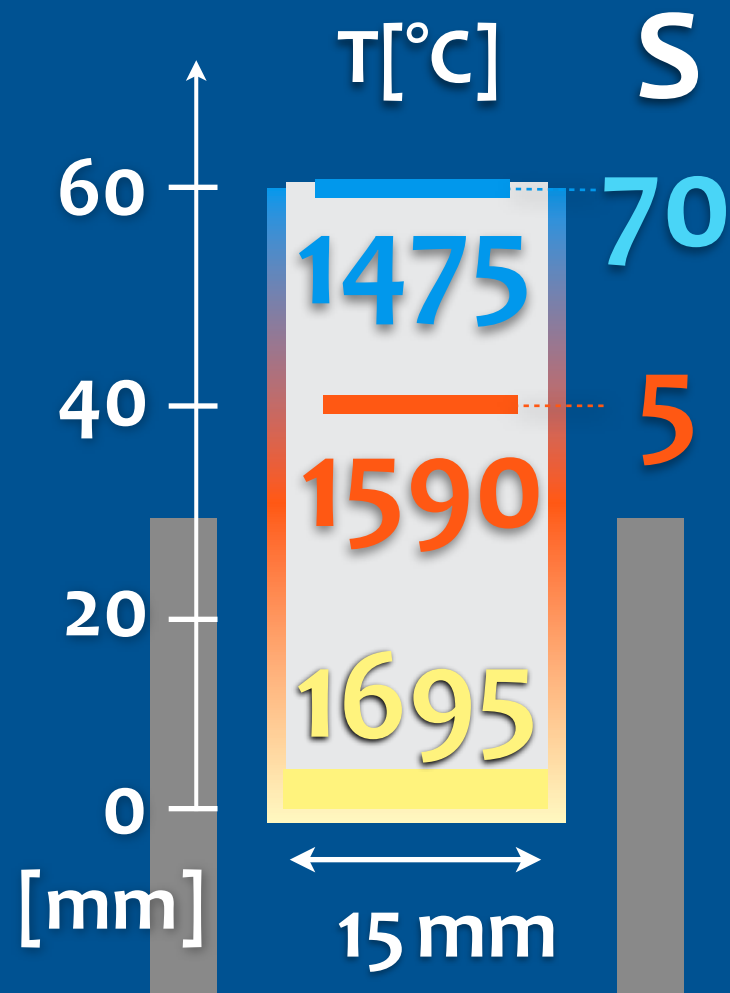
$$S2 = \frac{f_{in}}{f_{out}(T2)}$$

T _{gas} [°C]	T1 [°C]	S1	T2 [°C]	S2	t [h]
1695	1590	5	1475	70	9
1605	1490	9	1370	180	6,12,18
1535	>1435	<5	-	-	240
1505	1380	15	1260	330	120,360

Condensates at S=70

$P = 5 \times 10^{-5} \text{ Pa}$

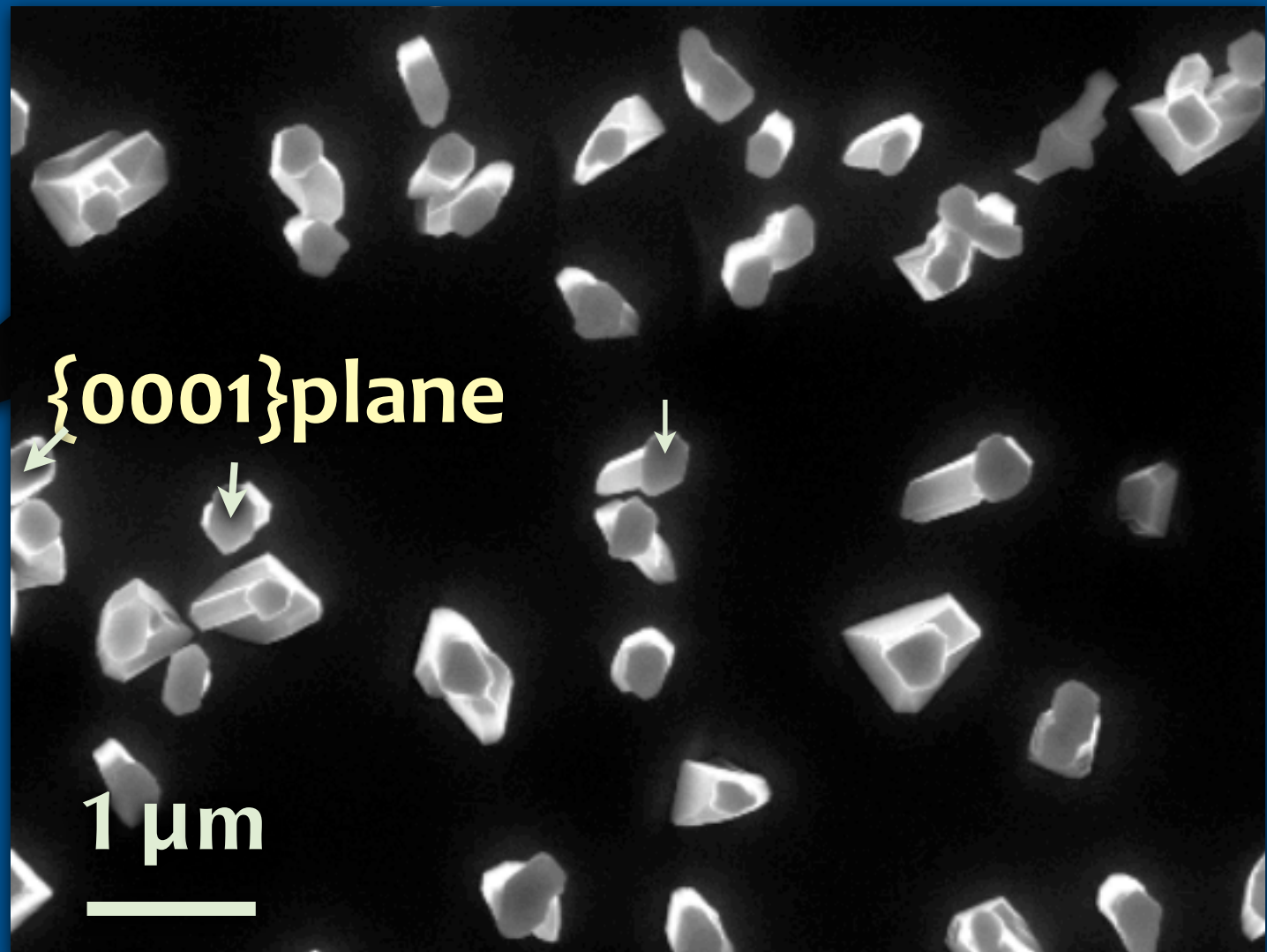
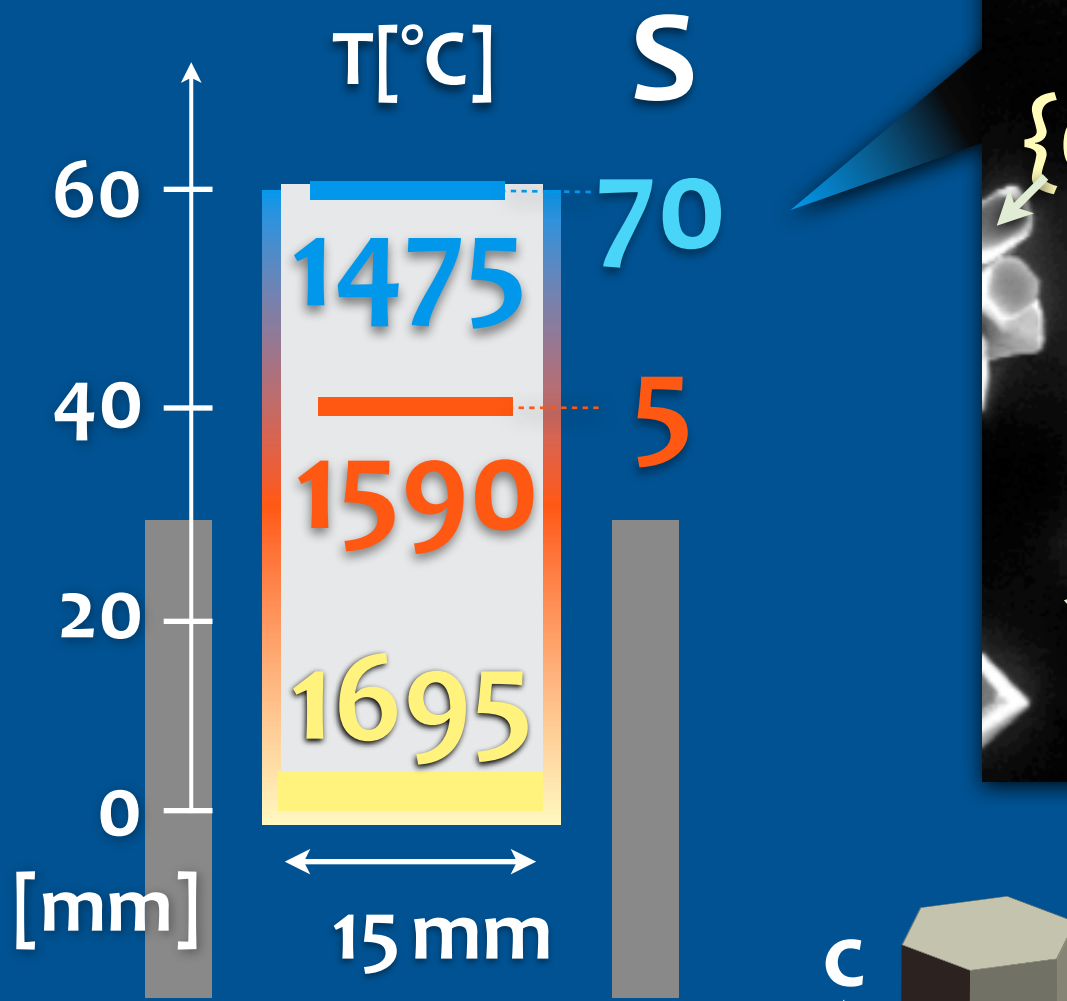
$t = 9 \text{ hrs}$



Condensates at S=70

$P = 5 \times 10^{-5} \text{ Pa}$

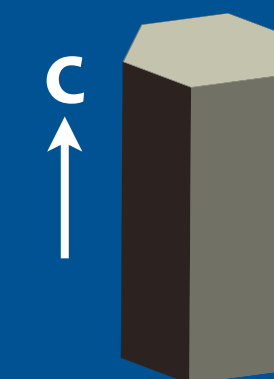
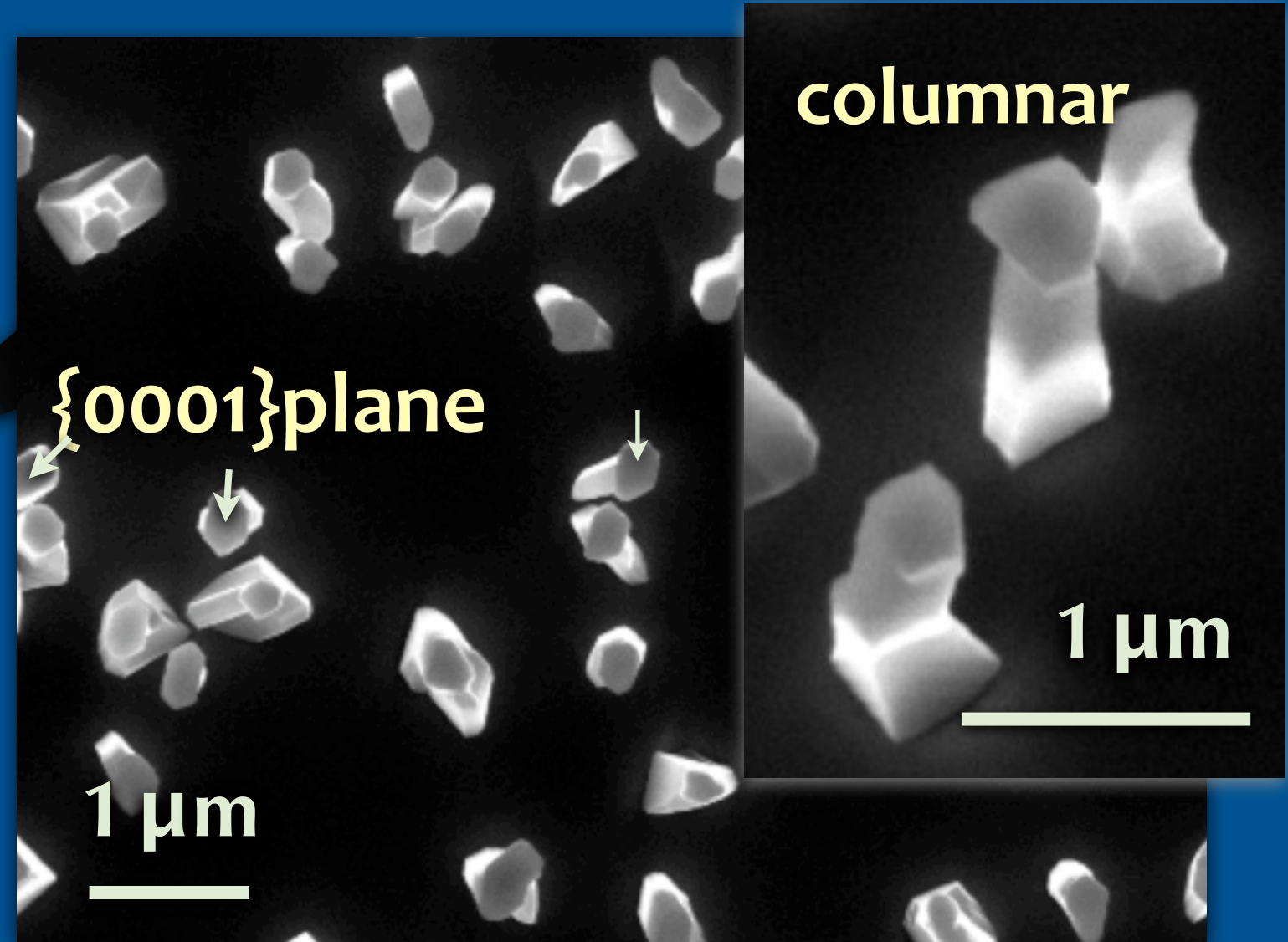
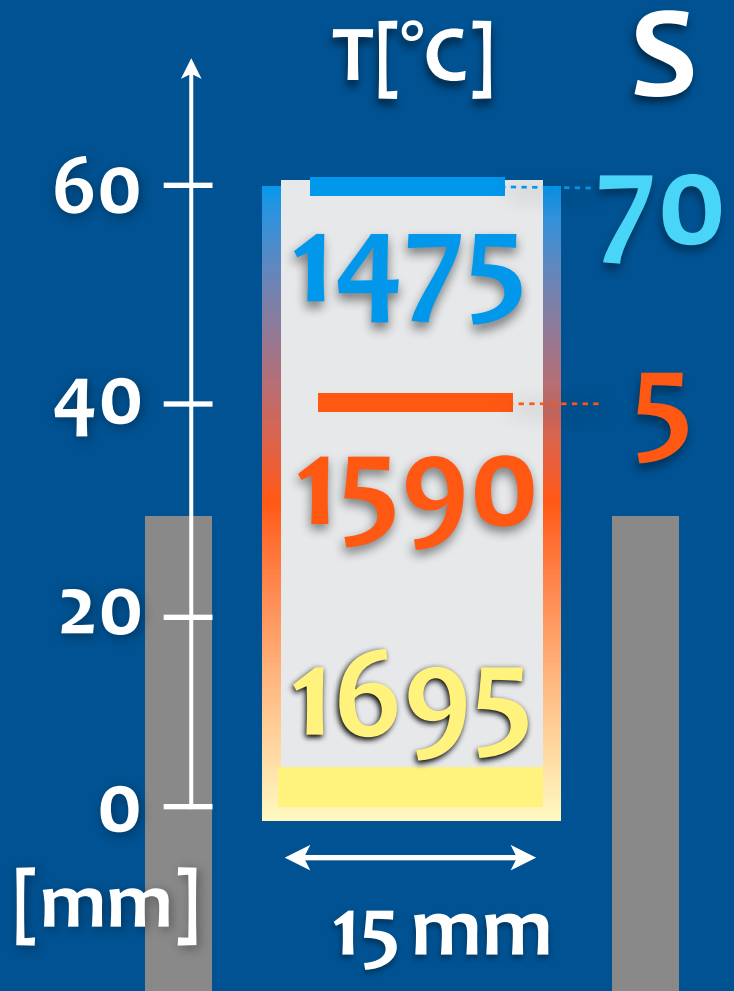
$t = 9 \text{ hrs}$



Condensates at S=70

P = 5×10^{-5} Pa

t = 9 hrs

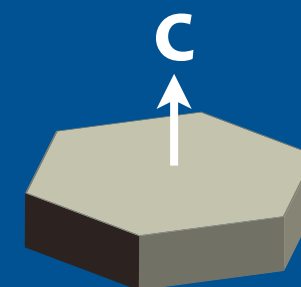
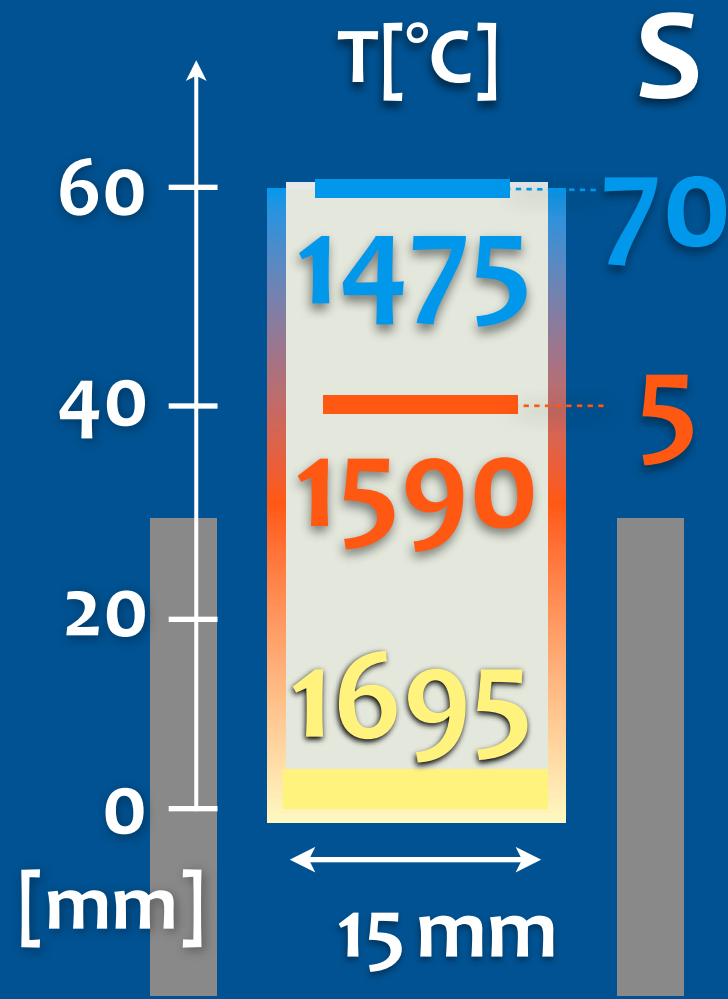


α-corundum elongating
along the c-axis ($\sim 0.3 \times 2$ μm)

Condensates at $S=5$

$P = 5 \times 10^{-5} \text{ Pa}$

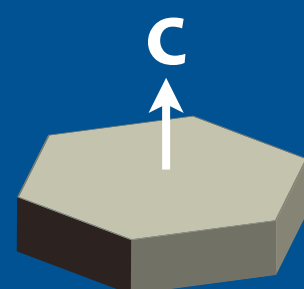
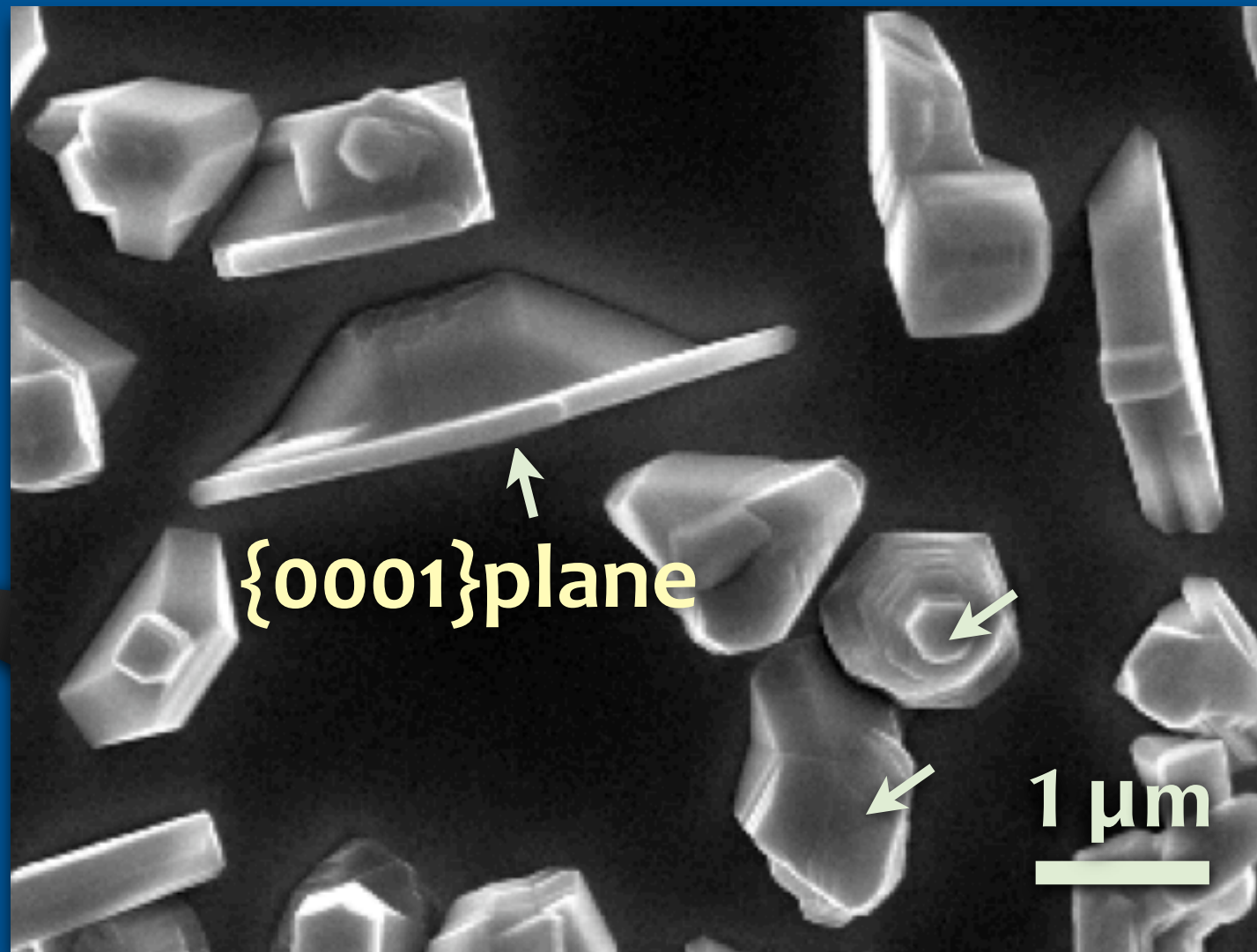
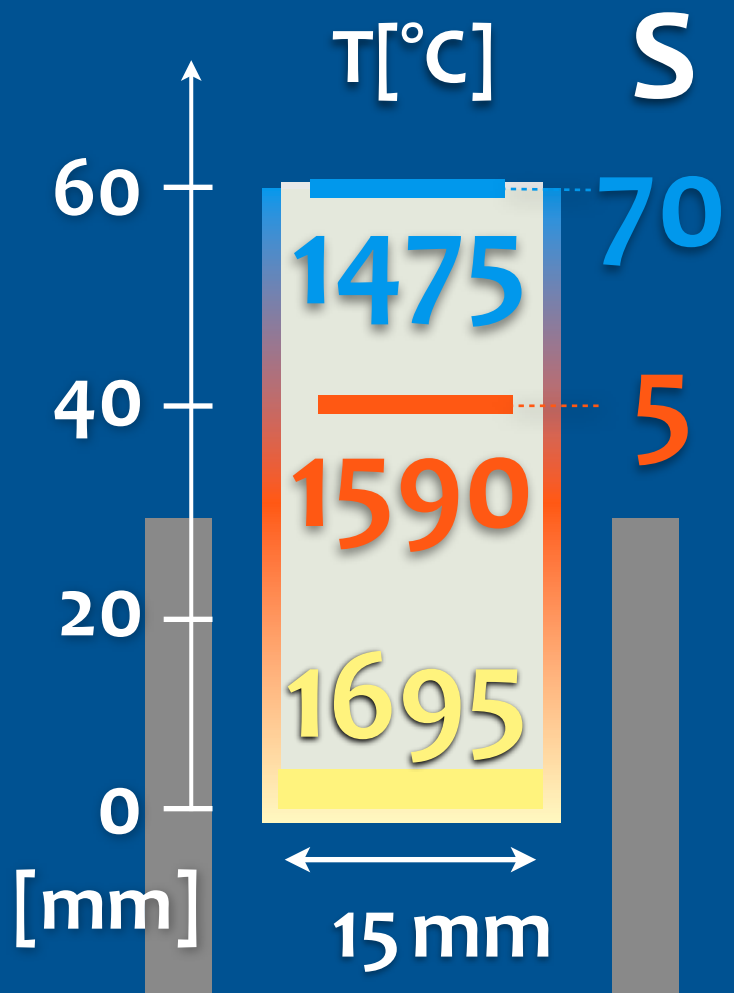
$t = 9 \text{ hrs}$



Condensates at $S=5$

$P = 5 \times 10^{-5} \text{ Pa}$

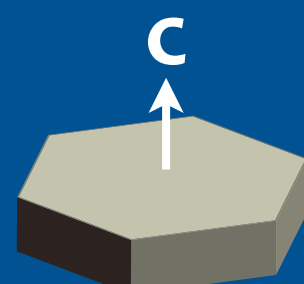
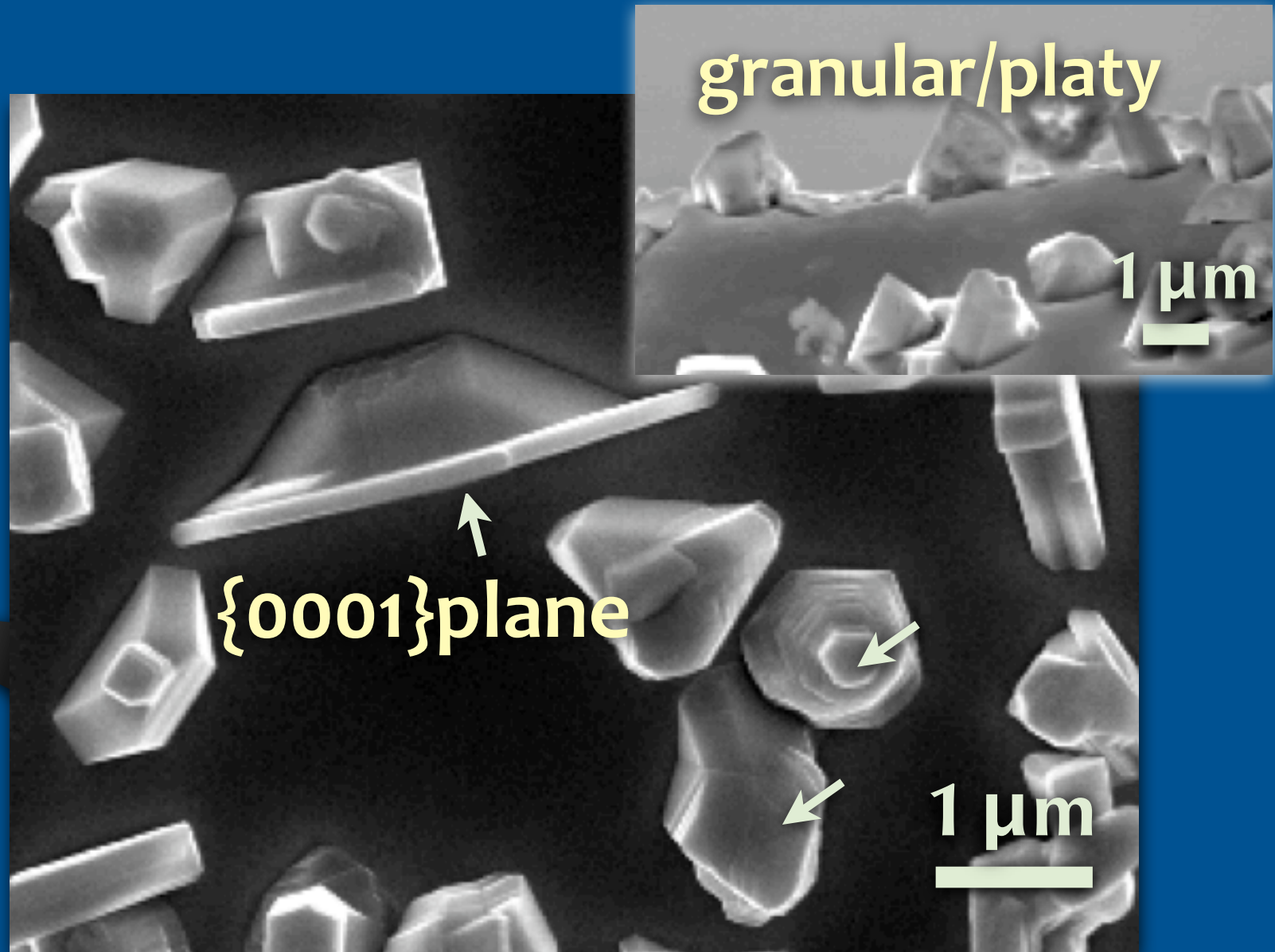
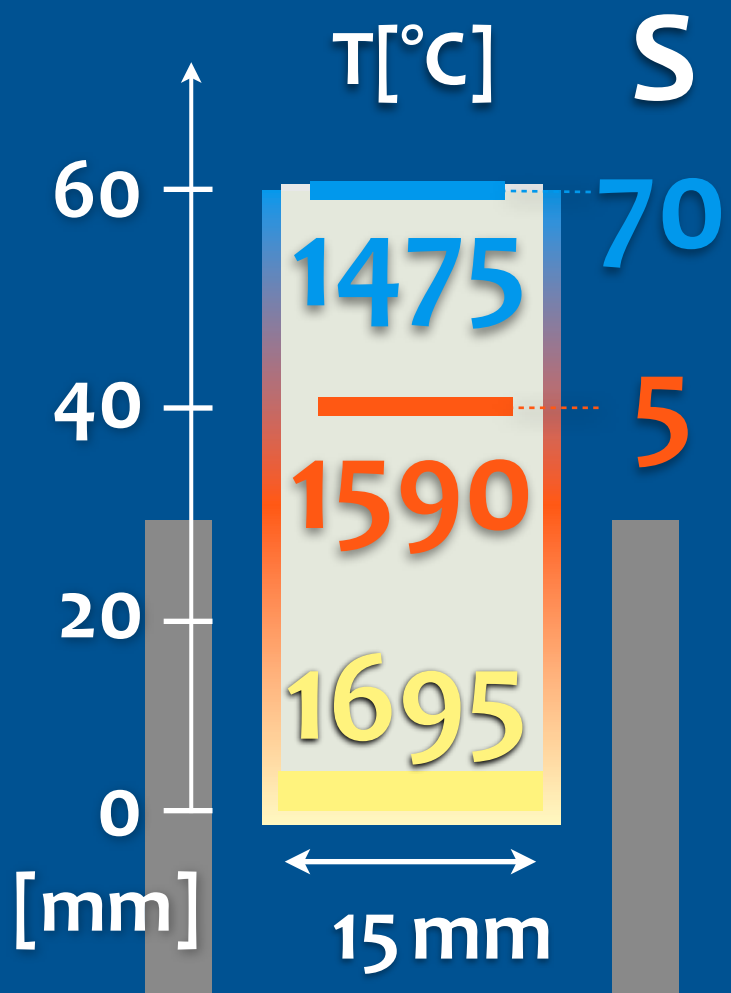
$t = 9 \text{ hrs}$



Condensates at $S=5$

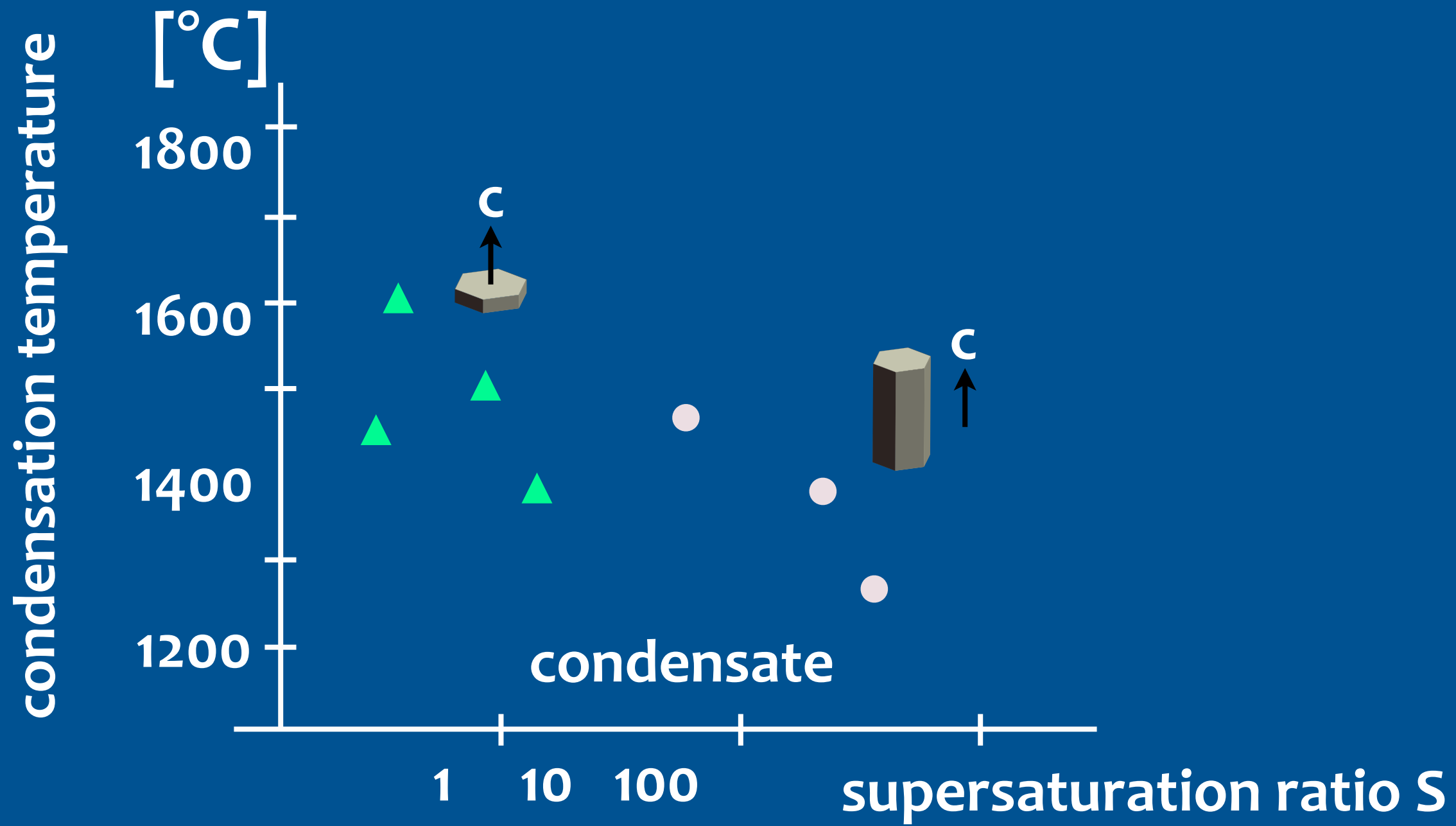
$P = 5 \times 10^{-5} \text{ Pa}$

$t = 9 \text{ hrs}$

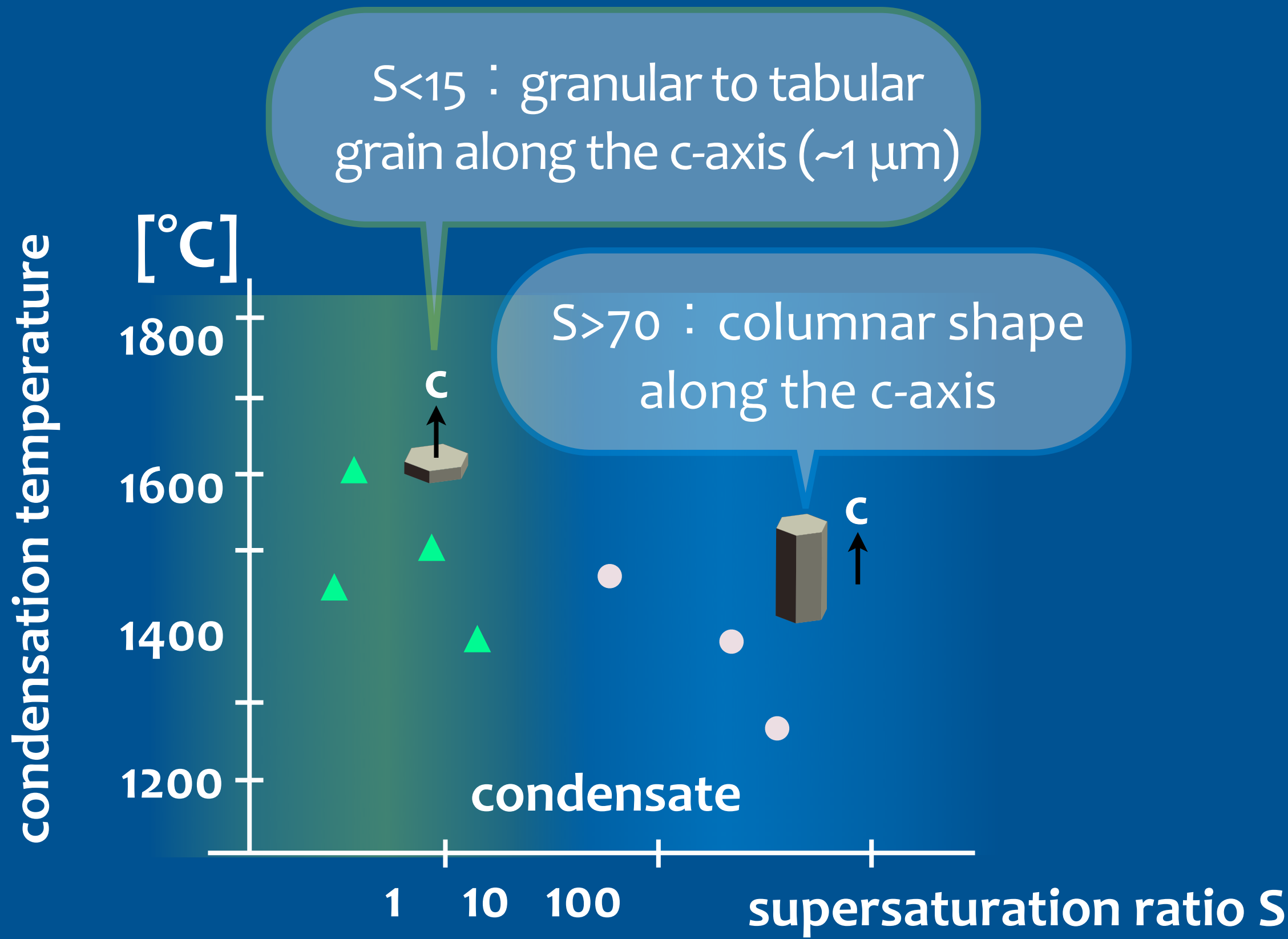


granular to tabular grain
along the c-axis ($\sim 1 \mu\text{m}$)

Growth form & condensation condition

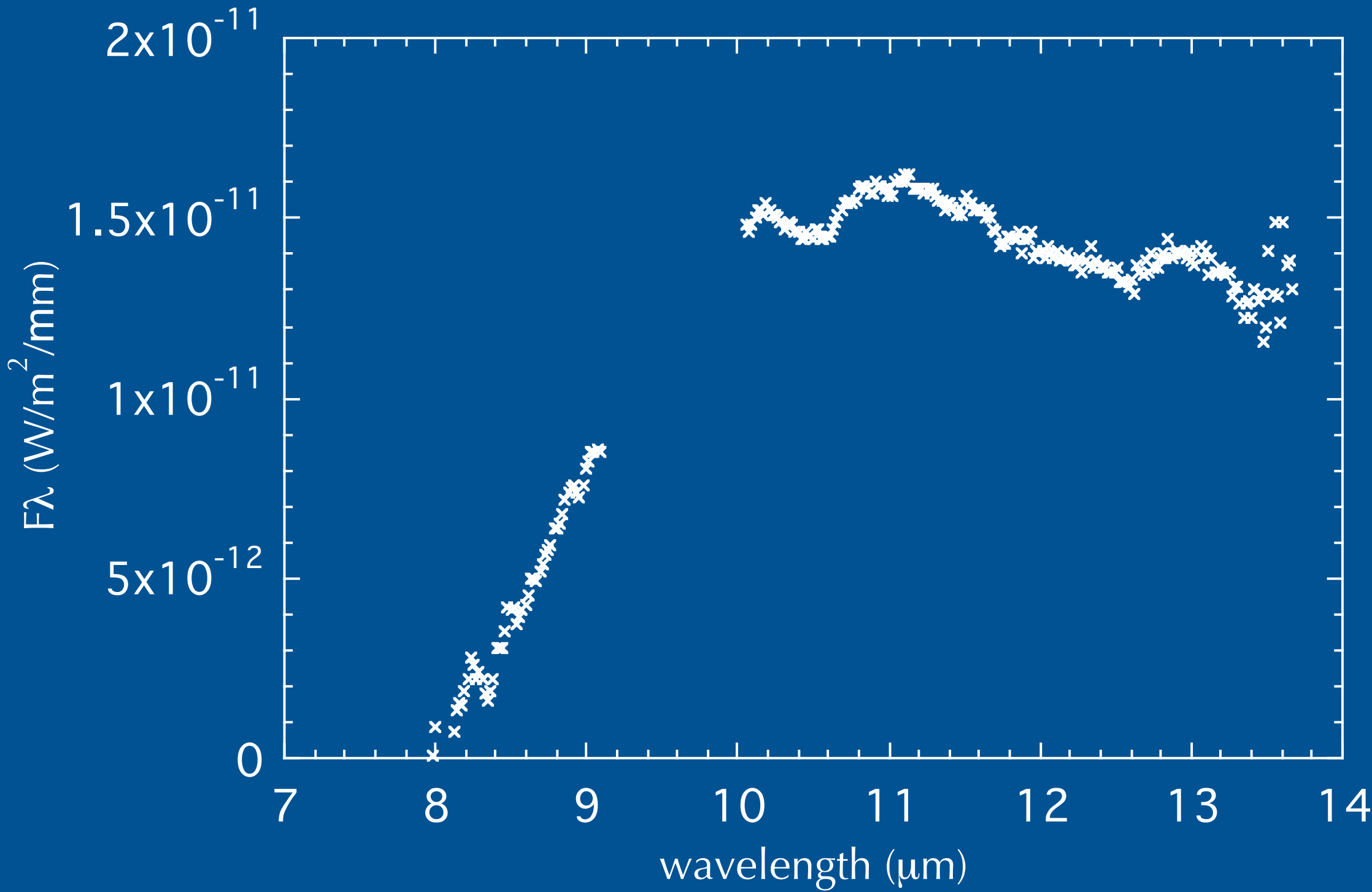


Growth form & condensation condition



the 13-micron feature of R-Cas

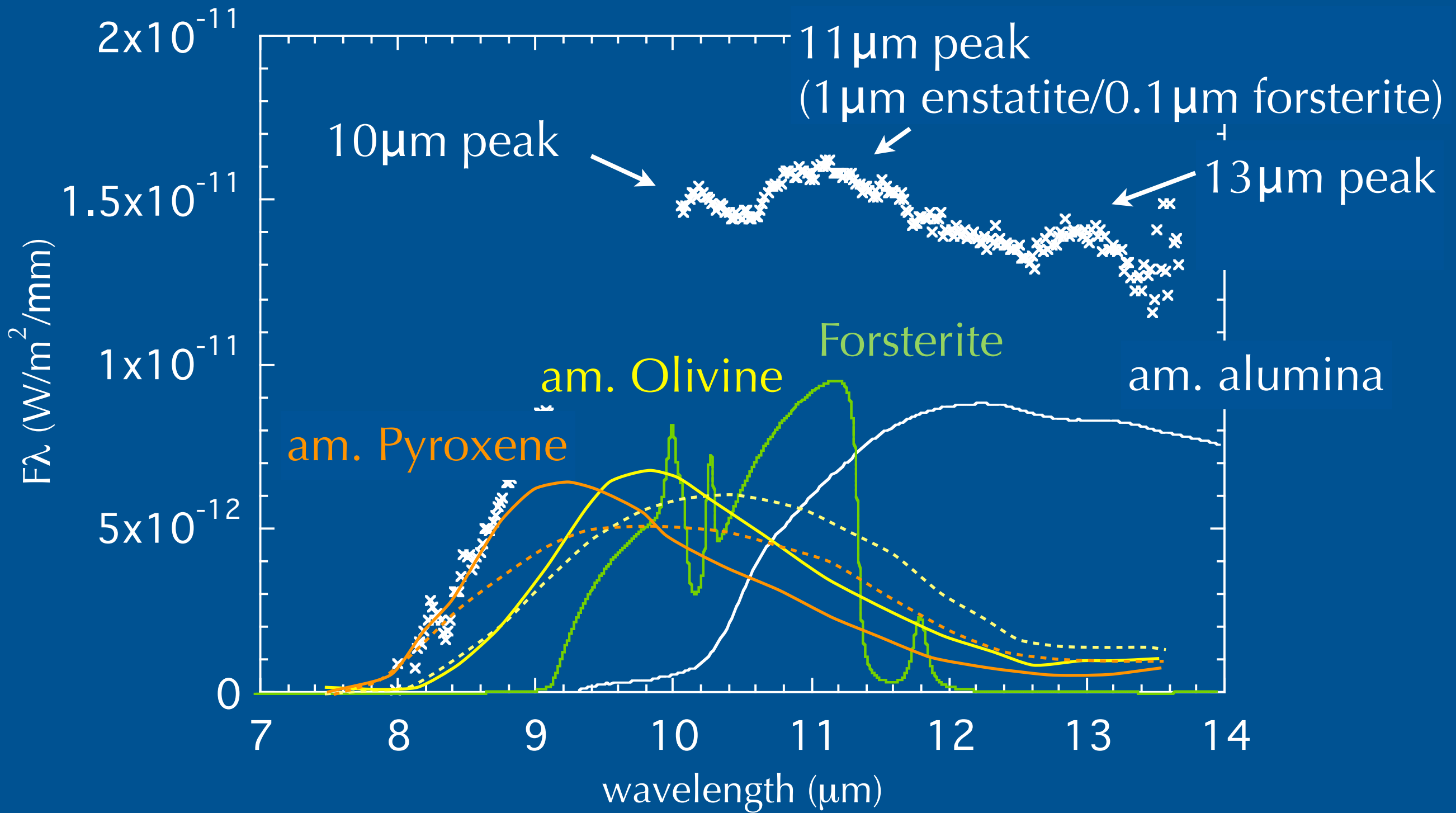
R Cas observed with Subaru/COMICS



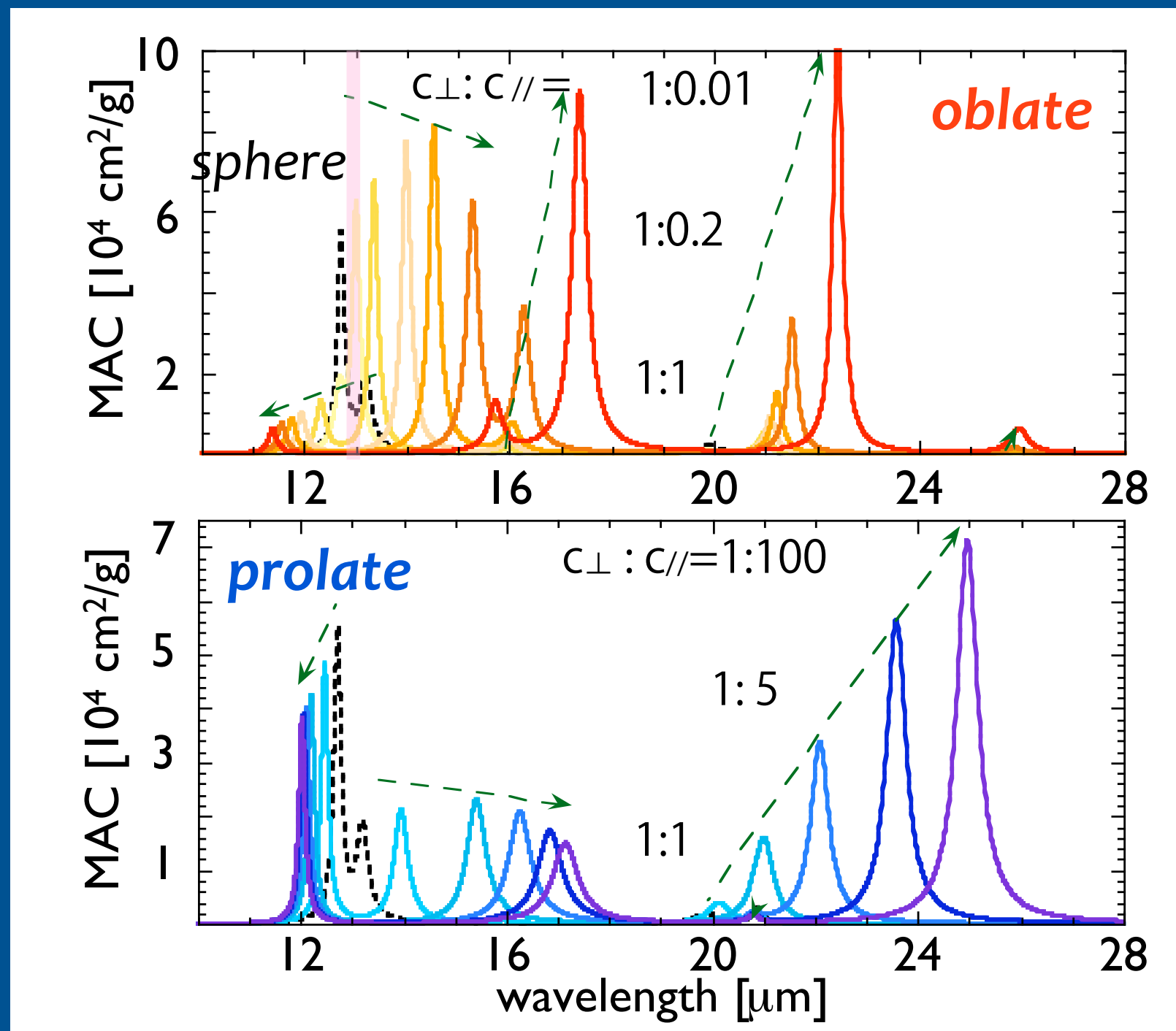
Takigawa et al. unpub. data

the 13-micron feature of R-Cas

R Cas observed with Subaru/COMICS



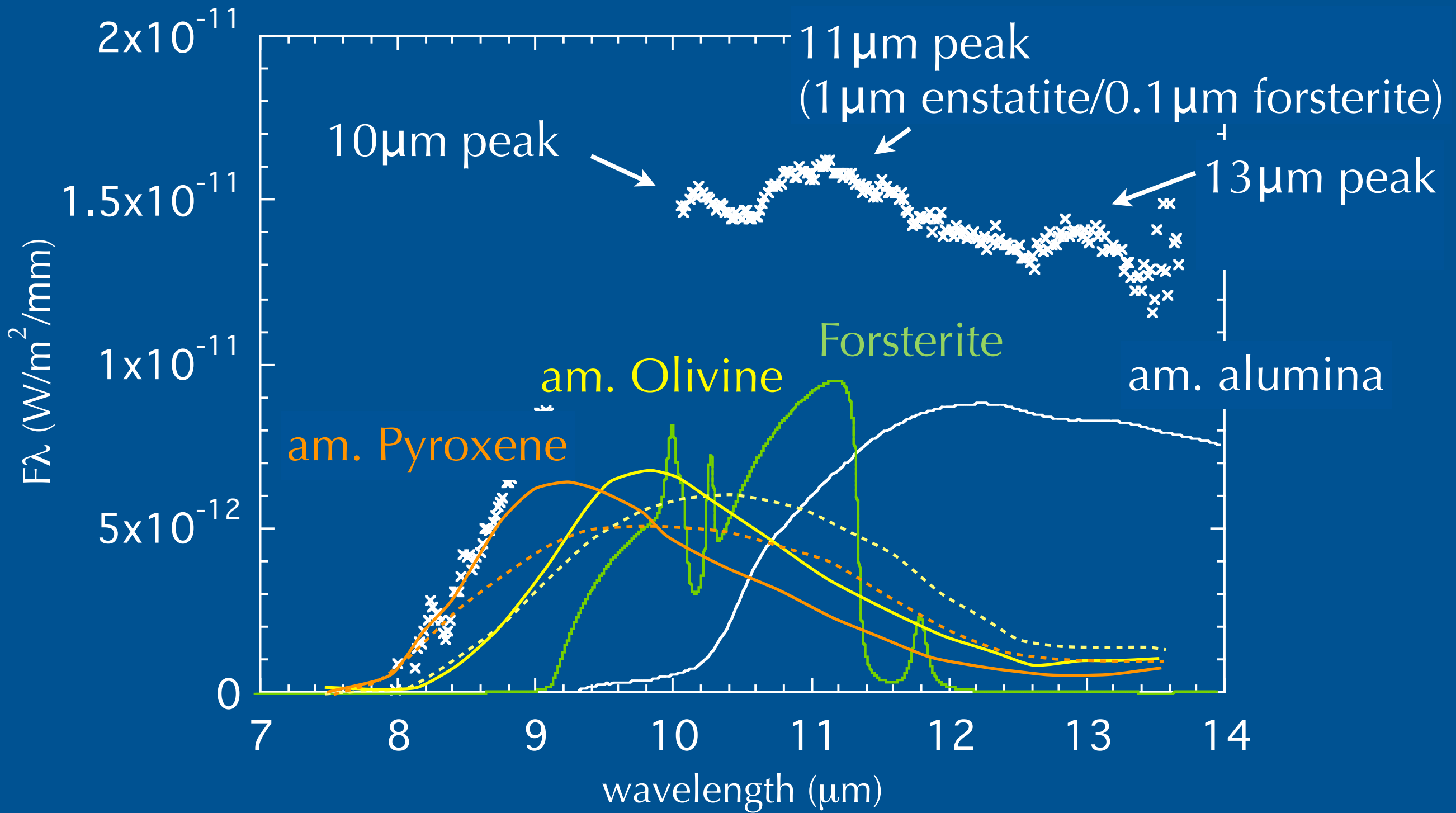
the 13-micron feature of corundum



Disk-shaped corundum grains along the c-axis ($c_{//}:c_{\perp}=2:3$)
- reproduce the 13- μm feature around O-rich AGB stars

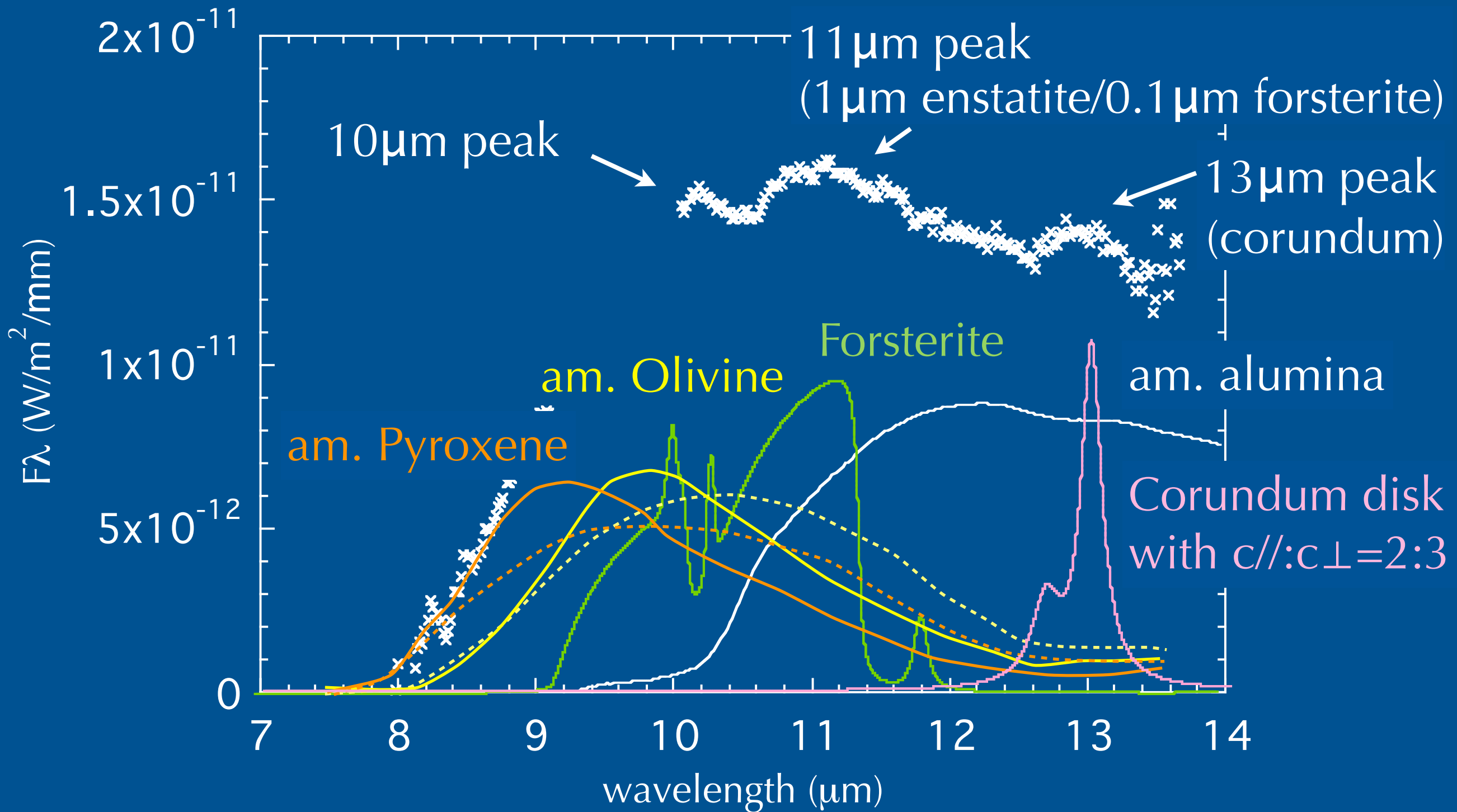
the 13-micron feature of R-Cas

R Cas observed with Subaru/COMICS



the 13-micron feature of R-Cas

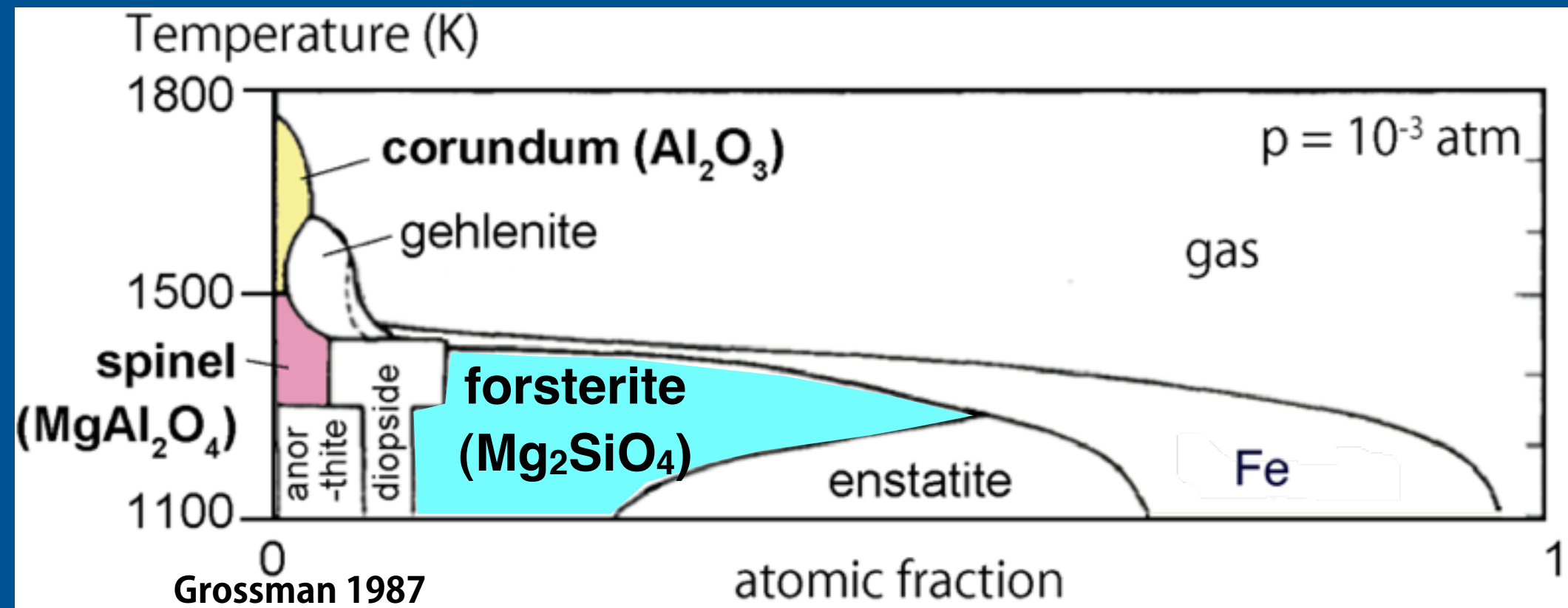
R Cas observed with Subaru/COMICS



Condensation of corundum

- Anisotropic
- Changes of crystallographically anisotropic shape cause observable changes of IR spectra
- Disk-shaped corundum explains the 13-micron feature

Spinel (MgAl_2O_4) formation experiments



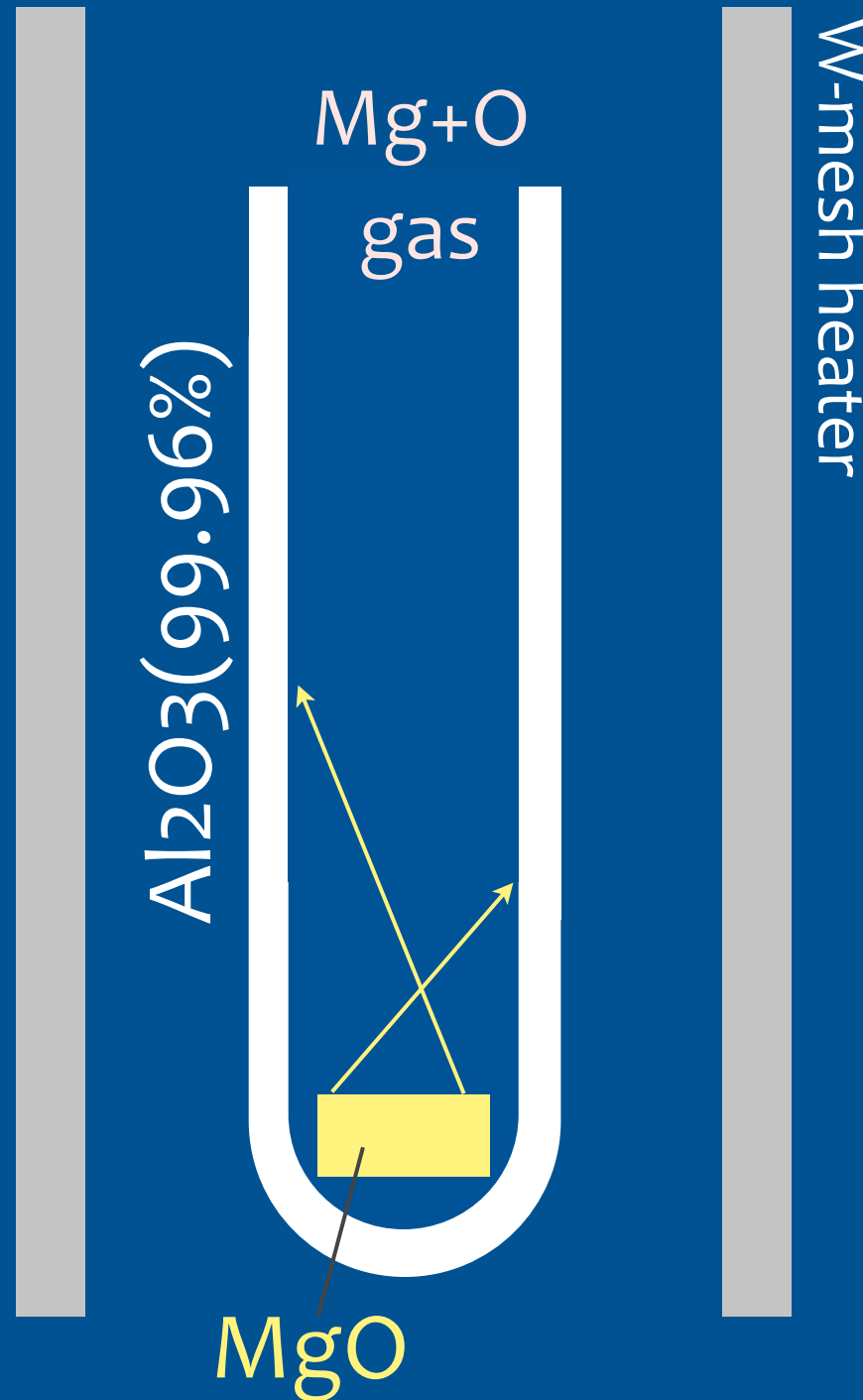
Corundum



Spinel

- Presolar spinel : evidence of spinel formation

Spinel (MgAl_2O_4) formation experiments



Reaction



Condition

$$T_{\text{gas}} = 1650^\circ\text{C}$$

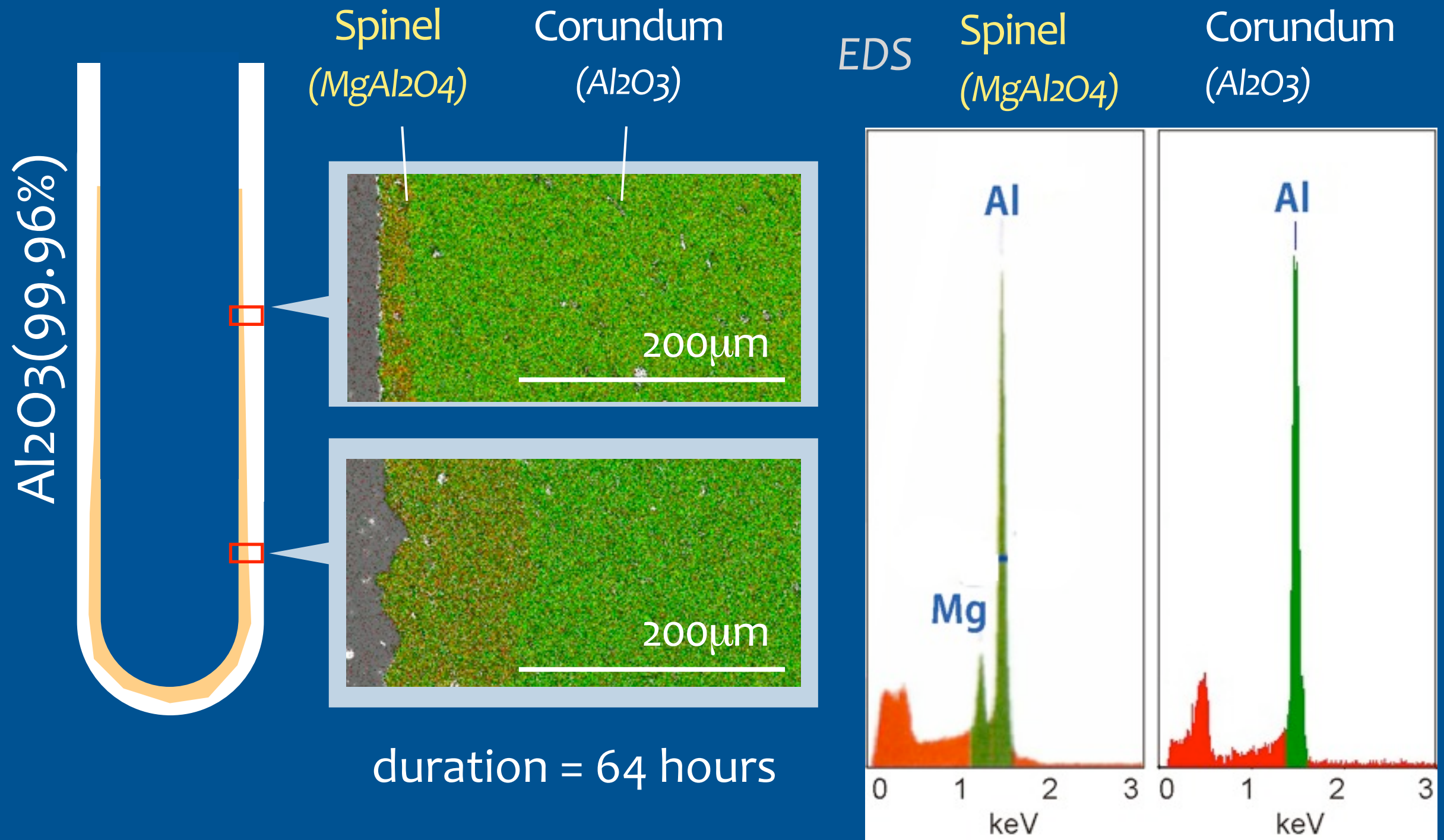
$$T_{\text{cond}} \approx 1550-1650^\circ\text{C}$$

duration = 24, 48, 64, 84, 254 hours

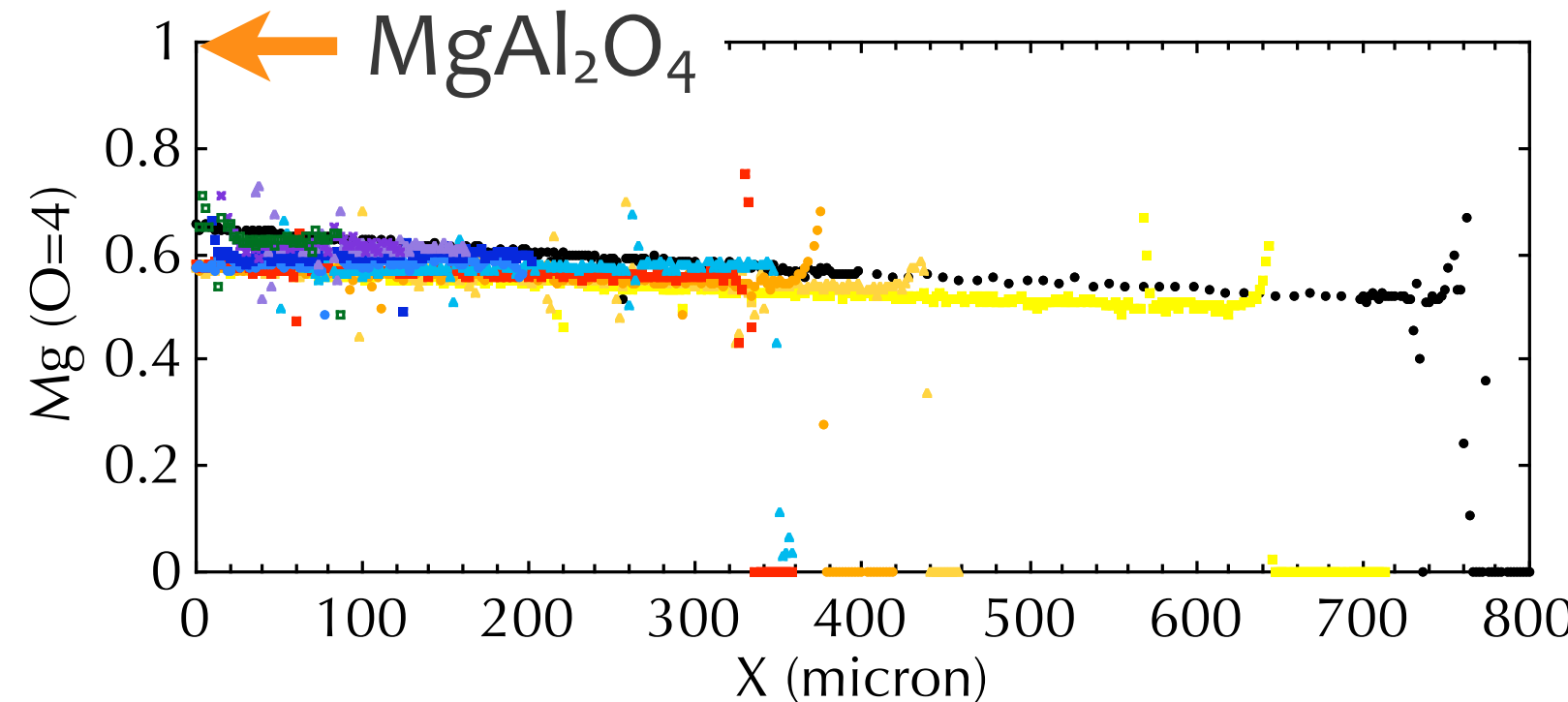
Analysis

SEM, EDS, EPMA, XRD, IR spectroscopy

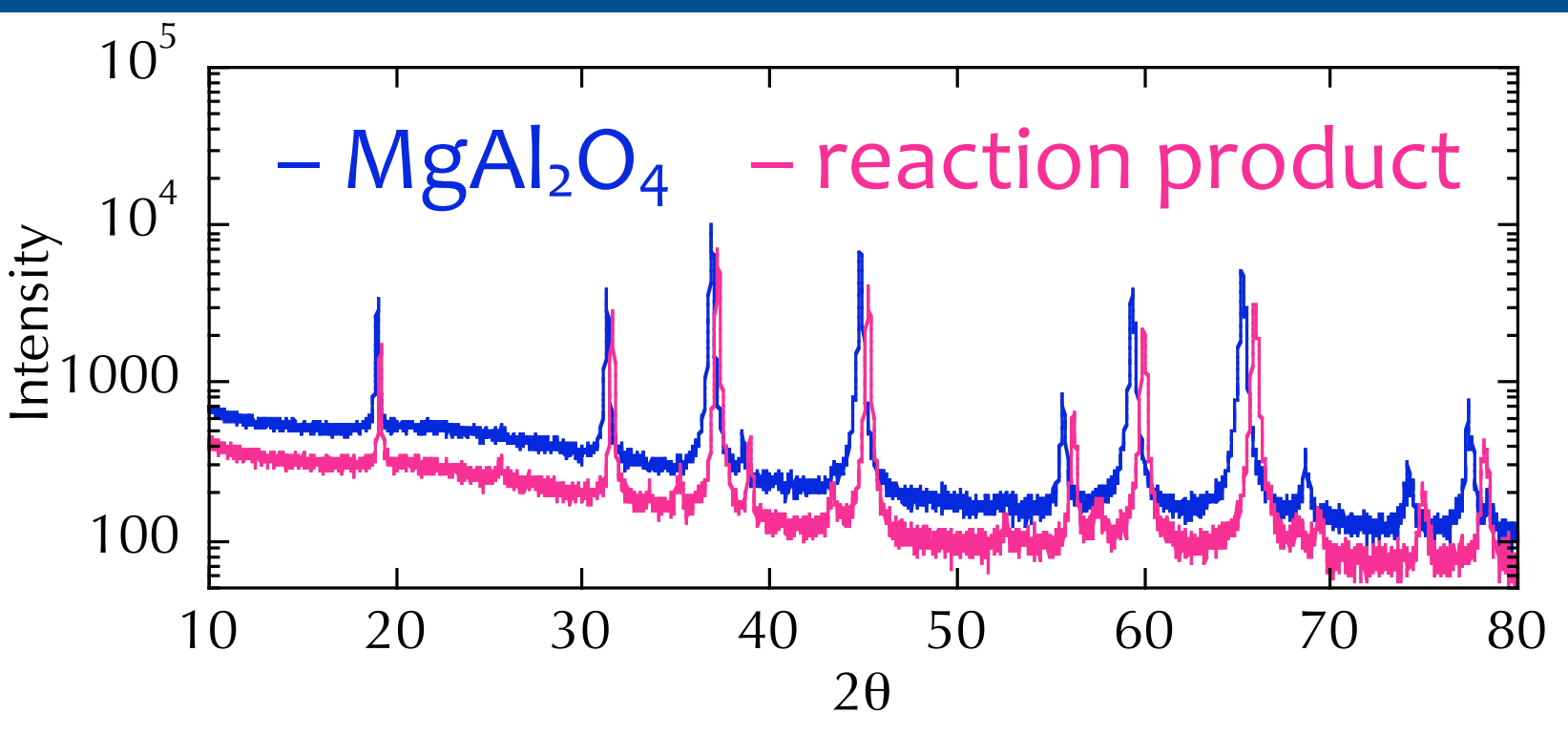
Reaction products



Reaction products



electron microprobe
 $Mg:Al = 0.6:2.3$ ($O=4$)
non-stoichiometric



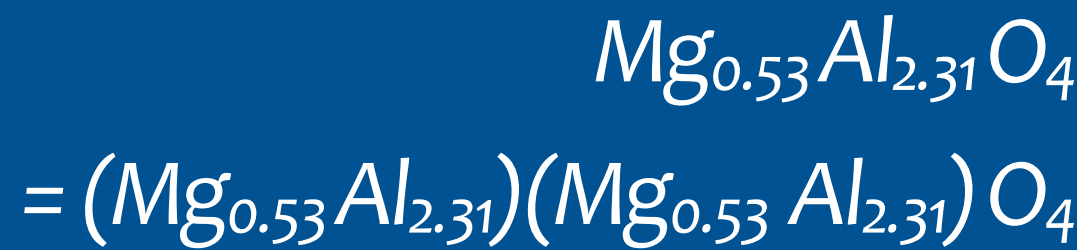
X-Ray Diffraction
lattice constant is $\sim 1\%$
smaller than that of
stoichiometric spinel

IR measurement

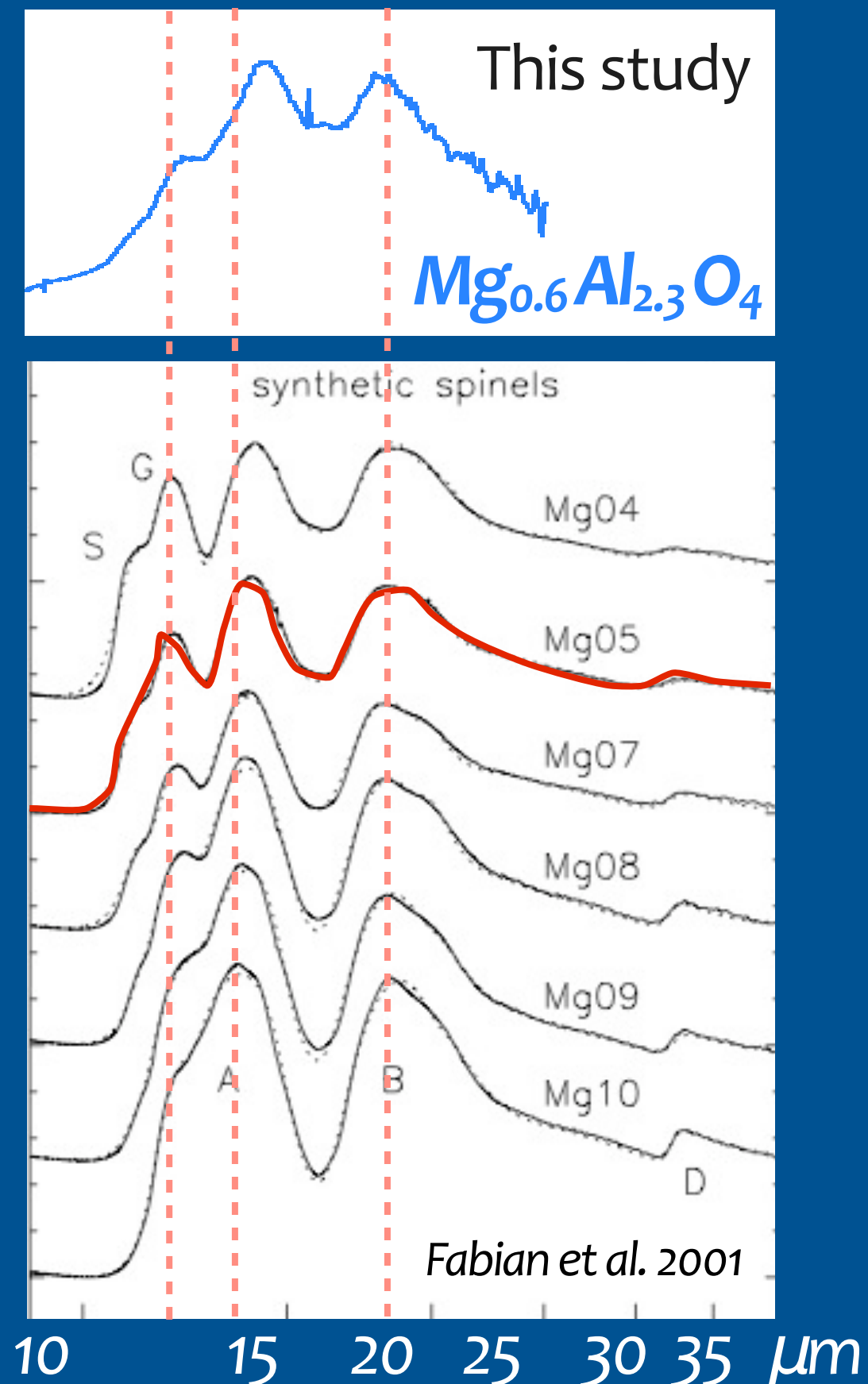
IR spectroscopy with KBr method

$Mg_{0.6}Al_{2.3}O_4$ formed at
 $\sim 1600^\circ C$ under low P

Comparison:
non-stoichiometric spinel synthesized
at 2050-2135°C (Fabian et al., 2001)



Different degrees of
disordering of cations ?
cf. more disordered at higher T



Conclusions

“Crystallographically anisotropic shape” is a key to link observed dust spectra and their formation conditions

- Forsterite evaporates anisotropically in H_2 gas depending on temperature and p_{H_2}
- Corundum condenses anisotropically depending on supersaturation ratio
- Crystallographically anisotropic shapes of forsterite and corundum can be deduced from spectral features
- IR measurement of non-stoichiometric spinel formed at low pressures is now being in progress